Article

Cell Reports

Purkinje cells translate subjective salience into readiness to act and choice performance

Graphical abstract

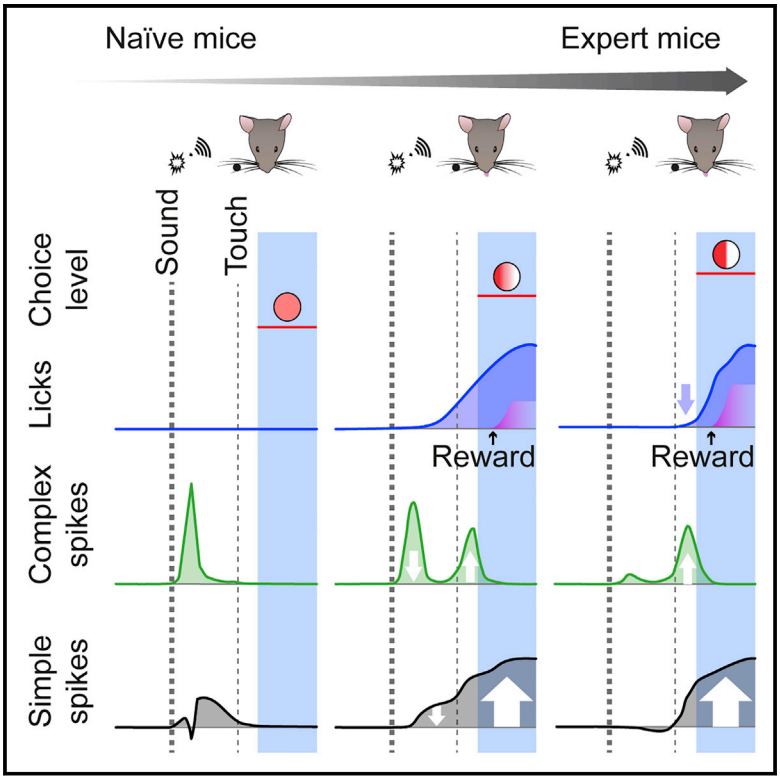

Authors

Lorenzo Bina, Vincenzo Romano, Tycho M. Hoogland, Laurens W.J. Bosman, Chris I. De Zeeuw

Correspondence

l.bosman@erasmusmc.nl (L.W.J.B.), c.dezeeuw@erasmusmc.nl (C.I.D.Z.)

In brief

Bina et al. describe that olivocerebellar neurons encode different types of sensorimotor and non-motor information during a discrimination task. Climbing fiber input relates to the perceived relevance of input and guides changes in simple spike output that, in turn, relate to choice performance and adaptation of movements.

Highlights

- Cerebellar encoding of sensorimotor and cognitive modalities depends on context
- Purkinje cell complex spike activity reflects perceived salience of sensory inputs
- Timing of complex spikes shifts when a readiness to act is required
- Simple spike modulation adheres to choice performance and motor activity

Bina et al., 2021, Cell Reports *37*, 110116
December 14, 2021
https://doi.org/10.1016/j.celrep.2021.110116

CellPress

Cell Reports

CellPress
OPEN ACCESS

Article

Purkinje cells translate subjective salience into readiness to act and choice performance

Lorenzo Bina,[1] Vincenzo Romano,[1] Tycho M. Hoogland,[1,2] Laurens W.J. Bosman,[1,3,*] and Chris I. De Zeeuw[1,2,*]
[1]Department of Neuroscience, Erasmus MC, Rotterdam 3000 CA, the Netherlands
[2]Netherlands Institute for Neuroscience, Royal Academy of Arts and Sciences, Amsterdam 1105 BA, the Netherlands
[3]Lead contact
*Correspondence: l.bosman@erasmusmc.nl (L.W.J.B.), c.dezeeuw@erasmusmc.nl (C.I.D.Z.)
https://doi.org/10.1016/j.celrep.2021.110116

SUMMARY

The brain selectively allocates attention from a continuous stream of sensory input. This process is typically attributed to computations in distinct regions of the forebrain and midbrain. Here, we explore whether cerebellar Purkinje cells encode information about the selection of sensory inputs and could thereby contribute to non-motor forms of learning. We show that complex spikes of individual Purkinje cells change the sensory modality they encode to reflect changes in the perceived salience of sensory input. Comparisons with mouse models deficient in cerebellar plasticity suggest that changes in complex spike activity instruct potentiation of Purkinje cells simple spike firing, which is required for efficient learning. Our findings suggest that during learning, climbing fibers do not directly guide motor output, but rather contribute to a general readiness to act via changes in simple spike activity, thereby bridging the sequence from non-motor to motor functions.

INTRODUCTION

The brain receives a continuous stream of sensory input, most of which is ignored. It can be a matter of life and death, however, to select those inputs that require attention: failing to act adeptly when confronted with a predator can be fatal. The salience of sensory inputs is not static, but rather depends on the ever-changing behavioral and environmental context of the animal; thus, the actions chosen in response to similar inputs can vary substantially over time. Selective attention is closely related to working memory and is widely considered to be organized by the forebrain in conjunction with the midbrain (Knudsen, 2018; Smith and Jonides, 1999; Buschman and Kastner, 2015). A putative involvement of the cerebellum in selective attention is unclear, as patients with cerebellar deficits do not necessarily have overt attentional deficits (Helmuth et al., 1997; Abdelgabar et al., 2019), whereas human brain imaging reveals cerebellar activity during both focused and shifting attention, even in the absence of movements (Le et al., 1998; Allen et al., 1997; Brissenden et al., 2018; Abdelgabar et al., 2019).

Classical theories explain cerebellar learning during reflex adaptation by supervised learning at the level of the output neurons of the cerebellar cortex, the Purkinje cells (PCs) (Marr, 1969; Albus, 1971; Ito, 2002a) (Figure 1A). Involvement of PCs in higher cognitive forms of learning remains a matter of ongoing research. PCs generate complex spikes (CSs) that occur at low frequencies and are evoked by activity of climbing fibers (CFs) originating from the inferior olive (IO), as well as simple spikes (SSs) that occur at higher frequencies and whose firing patterns are modulated by inputs from parallel fibers (PFs) and molecular layer interneurons (De Zeeuw et al., 2011; Zhou et al., 2014). CF activity controls synaptic plasticity of PF and molecular layer interneuron inputs, and the timing of CF activity may largely determine the direction of change in SS responsivity, which, in turn, may alter the motor response to sensory feedback (Herzfeld et al., 2018; Ohmae and Medina, 2015; Romano et al., 2018; ten Brinke et al., 2015; Yang and Lisberger, 2014; Ohtsuki et al., 2009). To understand the role of cerebellar learning in defined contexts, it is imperative to understand to what extent CF activity during acquisition can adapt to the salience of sensory inputs, entrained movements, and associated rewards. We would need to understand how CF activity impacts SS activity and whether the latter represents motor performance, non-motor performance, or both. Moreover, an equally important aspect that requires investigation is whether CSs and/or SSs relate to reward delivery and prediction (De Zeeuw, 2021; Heffley et al., 2018; Kostadinov et al., 2019; Tsutsumi et al., 2019).

We hypothesized that CF activity can encode the salience of sensory inputs, rather than their occurrence, and thereby provide a readiness to act signal, while SS modulation of the same PCs subsequently facilitates the required actions. We addressed this hypothesis by studying PC activity in the lateral cerebellum of mice while they learned to lick or abstain from licking based on the correct interpretation of distinct sequentially occurring sensory stimuli. We followed PC activity with electrophysiological recordings and calcium imaging throughout learning to reveal that both CS and SS patterns change bidirectionally. Using stimulation and interference paradigms, we demonstrate that these changes in PC activity enable effective learning of the sensory selection task, uncovering the participation of CFs in the acquisition and mediation of the salience of input signals, and the behavioral relevance of the subsequent SS modulations.

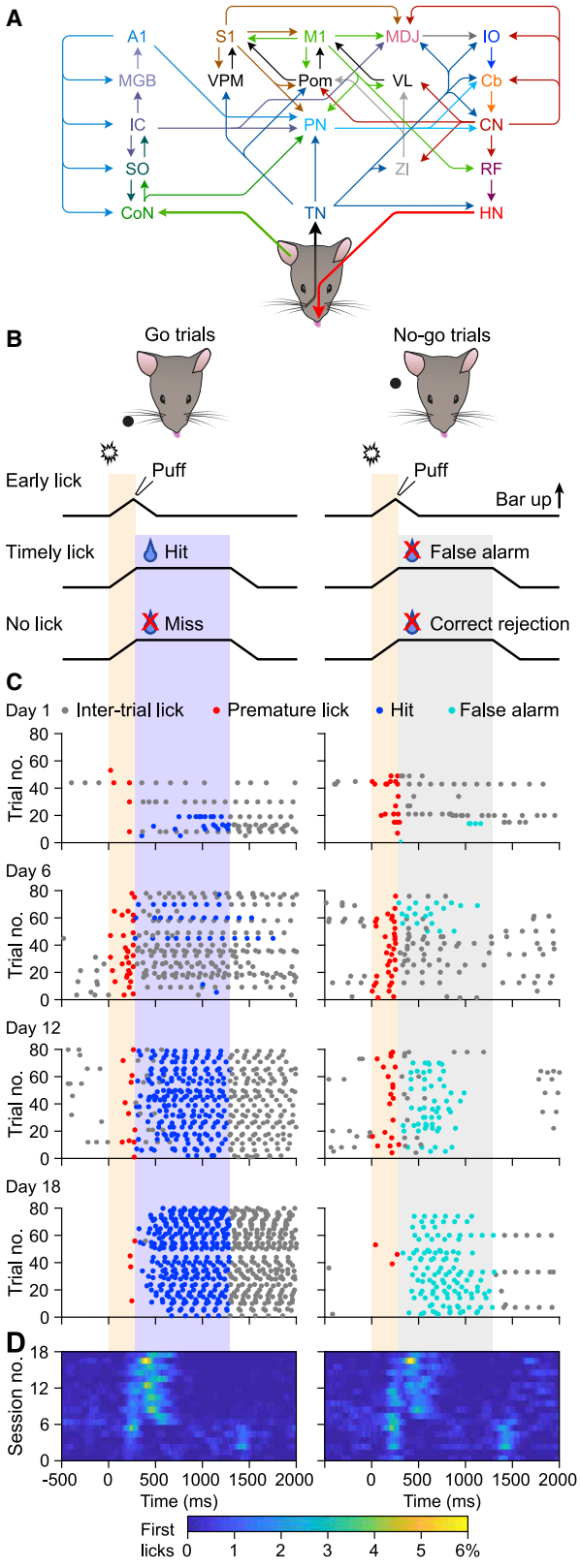

Figure 1. Training mice on a timed sensory selection task

(A) Main anatomical pathways involved in the task. A1, primary auditory cortex; Cb, cerebellar cortex; CN, cerebellar nuclei; CoN, cochlear nucleus; HN, hypoglossal nucleus; IC, inferior colliculus; IO, inferior olive; M1, primary motor cortex; MDJ, mesodiencephalic junction; MGB, medial geniculate body; PN, pontine nuclei; Pom, thalamic posteromedial nucleus; RF, reticular formation; S1, primary somatosensory cortex; SO, superior olive; TN, sensory trigeminal nuclei; VL, thalamic ventrolateral nucleus; VPM, thalamic ventral posteromedial nucleus; ZI, zona incerta.

(B) Between trials, a pole was rotated either below (go trials) or posterior to the whisker field (no-go trials). At trial start, a pneumatic valve elevated the pole, making a sound cue, followed by a 300-ms period (orange shade) during which licking triggered an aversive air puff to the nose and caused an immediate cessation of the trial. After the no-lick period, a response interval of 1 s followed (blue/gray shades). During the response intervals of go trials, mice could activate a water reward.

(C) At training onset, mice typically started to engage in the task by licking, initially not adhering to the different trial phases. During training, lick timing markedly improved.

(D) Heatmaps representing the averaged occurrences of first licks of bouts per 20-ms bin, showing first increased licking during the no-lick period and afterward a delay in the onset of lick bouts.

Data in (C) and (D) originate from the same exemplary mouse. See also Figure S1.

The timing of the observed increase in SS firing after learning suggests that cerebellar PCs may contribute to performing the correct choices as well as to optimizing the subsequent motor output. Our findings emphasize how the activity of both CSs and SSs adapts during learning, such that PCs can coordinate a context-dependent readiness to act at the appropriate time, thereby coupling motor with non-motor functions.

RESULTS

Training mice on a go/no-go paradigm with a no-lick period

To address how changes in PC activity contribute to learning a well-timed execution of a sensory selection task, we trained mice to decide whether to lick or not during a specific time interval upon perceiving a sequence of sensory stimuli. Licking at the correct moment triggered a water reward. Electrophysiological recordings at different stages of training allowed us to correlate PC activity with sensory perception, motor responses, and reward delivery. To this end, we engaged head-fixed mice on a go/no-go task (Figure 1B) for 18 daily sessions. Every trial began with an auditory cue identical for go and no-go trials (Figure S1B). This sound was created by a pneumatic valve lifting a pole into the whisker field. Around 300 ms later, the pole reached its maximal position, either within reach (go trials) or out of reach (no-go trials) of the facial whiskers. The mice were trained to suspend action until they could respond based upon perceiving whisker touch and, thus, to refrain from licking in the 300-ms interval during which the pole rose. The exact moment at which the pole could be felt varied between trials—depending on, among others, whisker position—but could be 200–250 ms after sound cue onset. Immediately after the pole reached its top position, a 1-s response interval ensued. To discourage responses during the no-lick period, early licks induced an aversive air puff to the nose and caused an immediate cessation of the ongoing trial.

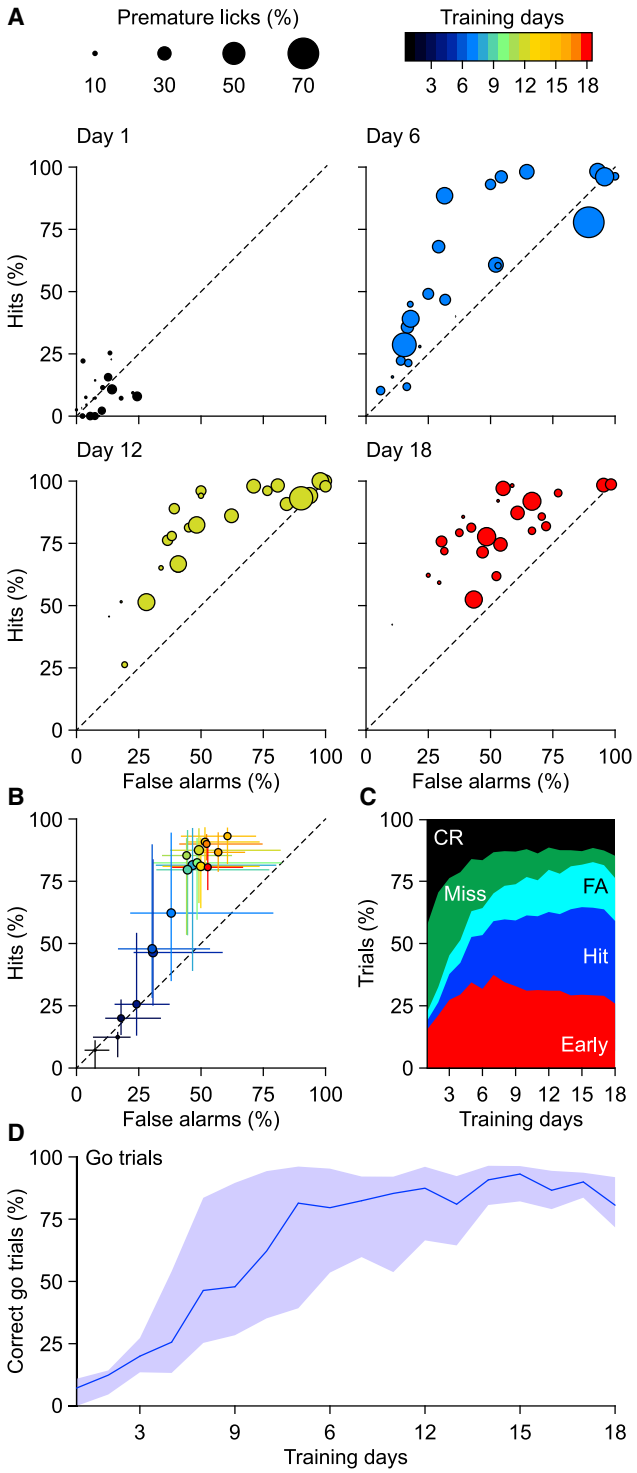

Figure 2. Learning to suspend licking takes more time than to learn to lick

(A) Scatterplots of the performance of all 24 mice, comparing the fraction of hits (y axis) and false alarms (x axis) during those trials that were not aborted due to licking during the no-lick period. The percentage of trials aborted due to early licking is indicated by the diameters of the circles. The 45° line indicates no discrimination between go and no-go trials.

(B) Median training performance. Days are color coded (see top of A).

(C) Averaged learning performance per trial type. CR, correct rejection; FA, false alarm.

(D) During learning, and regarding only trials without early licks, the median fraction of go trials during which mice engage in licking increased.

Bars (B) and shade (D) indicate IQR.

During a go trial without early licks, a water reward was triggered when licking occurred during the response window; the reward was not presented without prior action of the mouse. Rodents normally lick in bouts (Rahmati et al., 2014; Weijnen et al., 1984), and this was especially apparent after receiving a water reward (Figure 1C). Typically, mice first learned to engage in licking prior to withholding licking at undesired moments (Figure 1D).

Learning to suspend action takes longer than learning to act

Before training started, mice were familiarized with the setup and the lick port. Around training day 5, mice started to respond more often during go trials than during no-go trials. Early on, mice also licked relatively often during the no-lick period, triggering early termination of trials. Around training day 8, mice began to withhold licking until the start of the response window (Figures 2A–2C). Mice often reached a plateau level of performance after 2 weeks of training without further improvements. Training, therefore, ended after 18 days despite frequent mistakes. On the last training day, mice showed early licks during 26% ± 12% of the trials. In the trials without early licking, mice made 64% ± 7% correct choices (mean ± SD on day 18). In particular, during go trials, the percentage of correct responses increased during training from 7 (11)% to 81 (20)% (medians and interquartile ranges [IQRs]) (Figure 2D). As explained below, the error trials allowed us to discriminate between neural correlates of decision-making and those of motor control.

Distinct PC responses of naive and trained mice

To understand relations among CSs, SSs, and task performance, we performed electrophysiological recordings in lobules crus 1 and 2. The combination of sensory stimuli, choice performance (akin to decision-making), reward prediction and delivery, as well as motor action, made it challenging to determine how specific neuronal activity patterns might relate to distinct aspects of the task. Therefore, we systematically focused on one aspect at a time.

First, we concentrated on the impact of sensory input in naive mice that had not been familiarized to the lick port. Consequently, they did not lick and neither expected nor received water rewards. During go trials, the sound cue that signaled the start of the no-lick period was followed by a statistically significant CS response in 11 out of 24 (46%) recorded PCs, while whisker touch had this effect in only 4 PCs (17%). Among the PCs that showed at least one type of CS reaction, the sound-related response was stronger than the touch-related response ($p = 0.002$, Dunn's post hoc test after Friedman's ANOVA). The amplitude of sound-related responses did not differ between go and no-go trials ($p = 0.782$, Wilcoxon matched-pairs test; see Table S1 for more details on statistical analysis; Figures 3A–3C), as expected, since the sound cues were identical (Figure S1B).

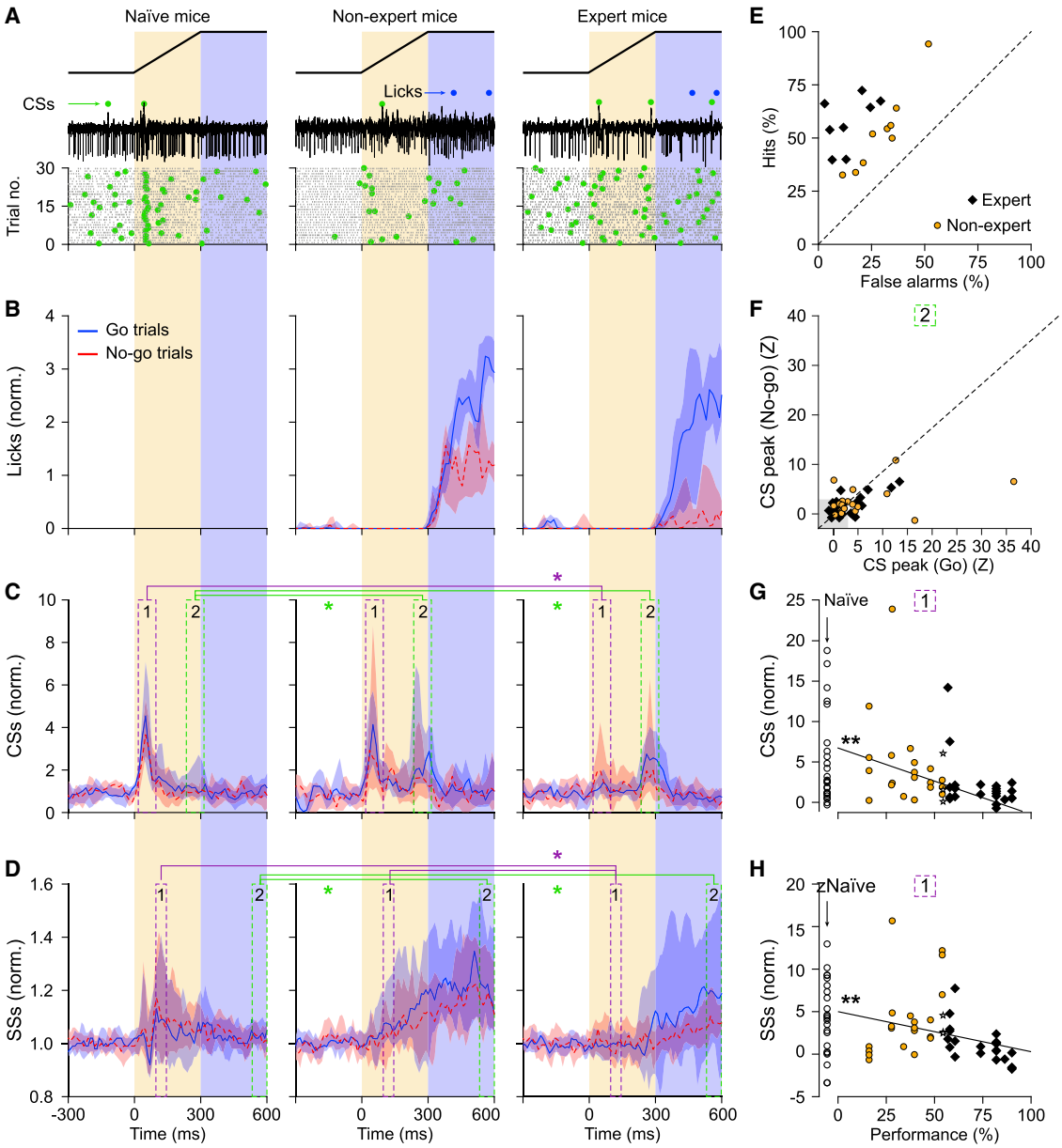

Figure 3. Distinct PC responses in naive and trained mice

(A) Representative recordings of PCs in crus 1 and 2 of a naive mouse, a trained mouse with relatively poor performance, and a trained mouse with expert performance. Scatterplots of CSs (green dots) and SSs (black dots).

(B) Peri-stimulus time histograms (PSTHs) of licks during go and no-go trials. Naive mice did not lick, and non-expert mice licked relatively often during no-go trials. Trials with early licks were excluded from this analysis. Lines indicate medians, and shades indicate IQR.

(C) PSTHs of PCs with a statistically significant CS modulation (16, 15, and 12 cells, respectively).

(D) As in (C), but for SSs. *$p < 0.05$, Friedman's ANOVA with Dunn's post hoc tests (see Table S1).

(E) Classification of expert and non-expert mice based on their licking during go versus no-go trials.

(F) At the level of individual cells, the amplitude of the CS peak during the second time interval—thus, following touch in go trials—is generally larger during go trials than during no-go trials (without touch).

(G) Performance was negatively correlated with the amplitude of the first CS peak ($r = -0.48$, $p = 0.001$).

(H) SS firing during the no-lick period (95–145 ms after trial start) was negatively correlated with performance ($r = -0.40$, $p = 0.006$).

In (G) and (H), n = 45 PCs, Spearman rank correlation tests. See also Figures S1–S4 and Table S1.

Next, we recorded from fully trained mice. Given heterogeneity in behavioral responses, we took a median split based on task performance, separating expert from non-expert mice (Figure 3E). We next analyzed the go trials only, excluding trials with early licks. It was evident that the ratio of CS responses following the acoustic and tactile cues was different. Expert mice showed reduced responses following acoustic cues and increased responses upon touch, whereas non-expert mice fired more CSs following acoustic than following tactile cues (Figure 3C; Table S1). Subsequently, we also performed a correlation analysis without subdividing the mice. This analysis of trained mice confirmed the relationship between differential CS patterns and choice performance ($r = -0.48$, $p = 0.001$, $n = 45$, Spearman rank correlation; Figure 3G). We further expanded our analysis to all recorded PCs, including those that did not show statistically significant CS modulation, yielding similar results (Figures S1A and S1C). Thus, we conclude that after training, CS timing correlated with preparation of decision-making.

CS firings during the first window of opportunity (i.e., following the sound cue) and those during the second window of opportunity (i.e., following the moment of the tactile cue during go trials) were distributed over the network. Some PCs participated mainly during the first peak and others during the second, while several PCs participated in both (Figures S2A and S2B). Although CS modulation was most prominent in the medial part of crus 1, response types were diffusely spread over crus 1 and 2 (Figure S2C).

The sound cue was identical for go and no-go trials (Figure S1B), and, accordingly, the amplitude of the sound-related CS peak did not differ significantly between go and no-go trials across the three groups (p between 0.339 and 0.782; Table S1). In trained mice, CS firing at the end of the no-lick period was more pronounced during go trials, when actual touch occurred, than during no-go trials, during which the whiskers were not touched. In non-expert mice, the peak amplitude of this second wave of CSs did not differ significantly between go and no-go trials ($p = 0.055$; Table S1), in line with their unreliable responses following touch. The difference was significant in expert mice, however ($p = 0.012$; see Table S1; Figure 3F). In terms of CS firing, the discrimination between go and no-go trials was, thus, especially good in expert mice, but even in these mice, a minority of PCs showed more CS activity during no-go trials than during go trials, demonstrating heterogeneity in PC behavior.

In naive mice, the sound cue was followed by a double-peaked SS response, with the second peak being more prominent and occurring directly after the initial CS response (Figures 3D, S1D, and S1E) and without significant differences between go and no-go trials (Table S1). In trained mice, SS modulation directly following the sound cue was suppressed, but it emerged during later stages of the trials. The maximal SS modulation occurring 95–145 ms after trial start—when naive mice had a clear peak in their SS firing—was inversely correlated with choice performance ($r = -0.40$, $p = 0.006$, $n = 45$, Spearman rank correlation; Figure 3H). During the response window of go trials, the SS rate was increased in trained versus naive mice (Figures 3D, S1D, and S1E), and this was particularly robust in crus 2 (Figure S2C). Remarkably, the differences in SS responses between go and no-go trials during the sensory discrimination window were imperfect in expert mice (Table S1), possibly implying that SSs did not primarily encode sensory information in expert mice. Thus, during training, both CS and SS responses changed, and the degree of change correlated with task performance.

PCs also encode licking

After studying sensory-evoked responses, we next studied tongue motor control and reward delivery. As naive mice did not lick during recordings, we included untrained mice that were accustomed to the lick port but not previously introduced to whisker stimulation. Unlike the first group of mice, untrained mice received water rewards at random moments during trials without the need to initiate licking first. Care was taken that untrained mice could sense the presence of water, even if they did not lick.

First, we aligned CSs to all licks. Of the 18 PCs recorded in untrained mice, 11 (61%) showed significant CS modulation (Figures S3A and S3B). Considering all cells, we found 4 to fire more CSs during protraction of the tongue and 14 during retraction (Figures S3C and S3D). This anti-phasic firing could also be observed in simultaneously recorded PCs in the same mouse (Figure S3E).

As in naive mice, CS firing in untrained mice was increased after the sound but not obviously following whisker touch (Figures S3H–S3J). Reward delivery triggered statistically significant CS firing in eight PCs, with a latency of ~200 ms (Figures S3O–S3Q). We noted a discrepancy between the relatively sharp tuning of CS firing after reward delivery and the variable lick timing (cf.Figures S3P and S3O, respectively). We conclude that CSs are more likely related to reward delivery than to licking. That these were, at least to some extent, different processes was also apparent from the finding that only a few PCs modulated their CS firing significantly around licking, sound, as well as reward presentation, while more cells related to only one or two of these stimuli, or even to none of these conditions at all (Figures S3K, S3L, S3R, and S3S).

SSs were also modulated during licking (Figures S3F and S3G) as well as following the sound cue (Figures S3M and S3N). A subset of PCs showed a decrease in SS firing after reward presentation (Figures S3T and S3U), just prior to the increase in CSs (Figures S3O–S3Q). Hence, CSs as well as SSs can relate to tongue movements and rewards, in addition to sensory stimulation.

To identify putative acoustic startle responses triggered by the sound cue, we made video recordings of the facial whiskers in 10 mice. In none of these did we find any indication for a fast, stereotypic movement at trial start (Figure S4), as would be expected if acoustic startle responses would be evoked.

CSs relate more to sensory stimuli, SSs more to licking

To further examine the role of PC activity in trained mice, we separated all trials with licking during the response window, whether go or no-go trials, from those without licking. To have a clear comparison, trials with licks during the no-lick period were excluded from this analysis. Sound-related CSs did occur,

albeit infrequently, and no significant difference was observed in the amplitude of the CS response between trials with and without licks ($p = 0.784$, $W = -37$, $n = 34$ PCs with statistically significant CS modulation, Wilcoxon matched-pairs test). In contrast, at the end of the no-lick period, significantly more CSs were observed when a mouse would lick afterward ($p < 0.001$, $W = 437$, $n = 34$, Wilcoxon matched pairs test; Figures 4A and 4B). CS activity did not remain elevated throughout the licking epoch, in contrast to SS activity that was systematically higher during, but not prior to, licking (95–145 ms [start of no-lick period]: $p = 0.812$, $W = -39$; 255–305 ms [end of no-lick period]: $p = 0.216$, $W = 199$; 545–605 ms [response window]: $p < 0.000$, $W = 577$, Wilcoxon matched-pairs tests; Figures 4A and 4B). Thus, the temporal pattern of increased CS firing followed by increased SS firing aligned temporally with the preparation and execution of the licking behavior, respectively.

We further refined this analysis by examining the hit trials, including all recorded PCs, as well as those that showed limited modulation in CS firing. Alignment on the sound cue revealed, as expected, a strong resemblance to Figure 4B, with CS firing peaking after trial onset (i.e., following the sound cue) and even more so just before the start of the response window (Figure 4C). However, CS modulation aligned on the timing of the first lick showed much more jitter than during the sensory-induced responses (kurtosis over 500-ms interval: $p = 0.002$, $W = 322$, $n = 31$ PCs with statistically significant CS peaks, Wilcoxon matched pairs test).

As the mice had to lick first to trigger a reward, the first lick was unrewarded. Given the potential importance of CSs for reward expectation (Heffley and Hull, 2019; Heffley et al., 2018; Kostadinov et al., 2019; Tsutsumi et al., 2019), we repeated this analysis by aligning the CSs on the second lick—thus, the timing of reward detection. This did not reveal a clear coupling between CS timing and reward delivery (Figure 4E). A further exploration of the putative role of CS firing in reward expectation in relation to our paradigm is provided in Figure 5.

Next, we analyzed the impact of CS firing prior to licking onset by comparing individual trials in which a CS occurred during the no-lick period to find the chance of licking to be unrelated to CS firing after either the sound or the tactile cue (Figure S5). Thus, although at the level of individual mice, the timing of CS firing can be related to the preparation of choice performance (Figure 3G), this does not hold at trial level when considering individual PCs. This could indicate that CS encoding is more a network than a single-cell phenomenon, compatible with an instructive role for CSs in guiding SS plasticity (Gao et al., 2012).

In contrast, in trained mice, SS modulation related more to licking than to the sensory cues (Figures 4C–4E), in line with our conclusion from Figure 3H. It was apparent, however, that more SSs followed the second lick—thus, when the mice could sense reward delivery—during rewarded than during unrewarded lick bouts ($p = 0.007$, $W = 129$, $n = 19$ PCs, Wilcoxon matched-pairs test; Figures S5C and S5D).

As increased SS firing precedes licking onset (Figures 3D and 4D), we wondered to what extent SSs could be related to the decision whether to lick in response to the sensory cues. To this end, we compared SS firing around spontaneous, unrewarded lick bouts in untrained mice to that during hit trials of trained mice. During hit trials, the increase in SS firing started substantially longer before the start of licking than during spontaneous bouts (spontaneous: −50 [148] ms, response: −210 [130] ms, medians [IQR], $p < 0.001$, $U = 74.5$, Mann-Whitney test, 14 versus 33 PCs; Figures 4F and 4G). This time lag was shorter in expert mice ($r = 0.389$, $p = 0.025$, $n = 33$ PCs, Spearman rank correlation test; Figure 4H). SS firing prior to the motor response may, therefore, contribute to choice performance.

Changing SS firing during the no-lick period affects choice performance and licking

Given that SS firing during the no-lick period was associated with choice, and as SS firing in crus 1 and 2 is related to licking (Bryant et al., 2010), we addressed whether a change in SS firing could affect lick timing as well as choice performance. *Pcp2-ChR2* mice have PC-specific expression Channelrhodopsin, allowing optogenetic SS stimulation and creating transient disruption of cerebellar nucleus neuron firing (Figures S6A and S6E) (Romano et al., 2018; Witter et al., 2013; Lindeman et al., 2021).

Optogenetic stimulation in crus 1 and 2 in trained mice during the no-lick period reduced the number of licks during the period of stimulation, effectively delaying licking onset (reduction in number of licks: $p = 0.007$, $t = 3.503$, $df = 9$, paired t test; Figures S6A–S6D). Optogenetic stimulation during this period affected specifically the outcomes of go trials (go: $p = 0.008$, $t = 3.358$; no-go: $p = 0.581$, $t = 0.572$, $df = 9$, paired t tests). In contrast, optogenetic stimulation during the response window did not alter ongoing licking ($p = 0.887$, $t = 0.146$, $df = 9$, paired t test; Figures S6E–S6H) and did not affect choice performance (go: $p = 0.749$, $t = 0.330$; no-go: $p = 0.630$, $t = 0.499$, $df = 9$, paired t tests). Thus, the decision whether and when to lick was affected by optogenetic stimulation during the period in which the decision to lick was made, while ongoing motor behavior was not affected.

Cerebellar activity is context dependent

During the sensory selection paradigm, CS firing was related to the delivery of a water reward in untrained mice (Figures S3P and S3Q) but not apparently so in trained mice (Figure 4E). Given the clear relation between CS firing and reward expectancy following associative learning (Kostadinov et al., 2019; Heffley et al., 2018; Tsutsumi et al., 2019; Larry et al., 2019), we studied this topic more extensively. We trained a set of mice on the "normal" paradigm, but during recording sessions, we withheld rewards (WR) on 20% of go trials and allowed mice to trigger a reward on 20% of no-go trials. These confounding trials were randomly distributed over the session, and the mice lacked *a priori* knowledge of whether a trial followed the normal or the deviant rules for reward. Probably largely because of these confounding trials, the performance of the mice during these sessions was relatively poor and, therefore, generally similar to that of the non-expert mice during experiments without confounding trials (Figure 5E).

CS firing peaked after the sound cue in all trials, and even more upon touch during go trials, but not during the response windows of any type of trial (Figures 5A–5D). As violations of the reward rules became evident during the response window, this absence of CS modulation indicates that neither WRs during a subset of

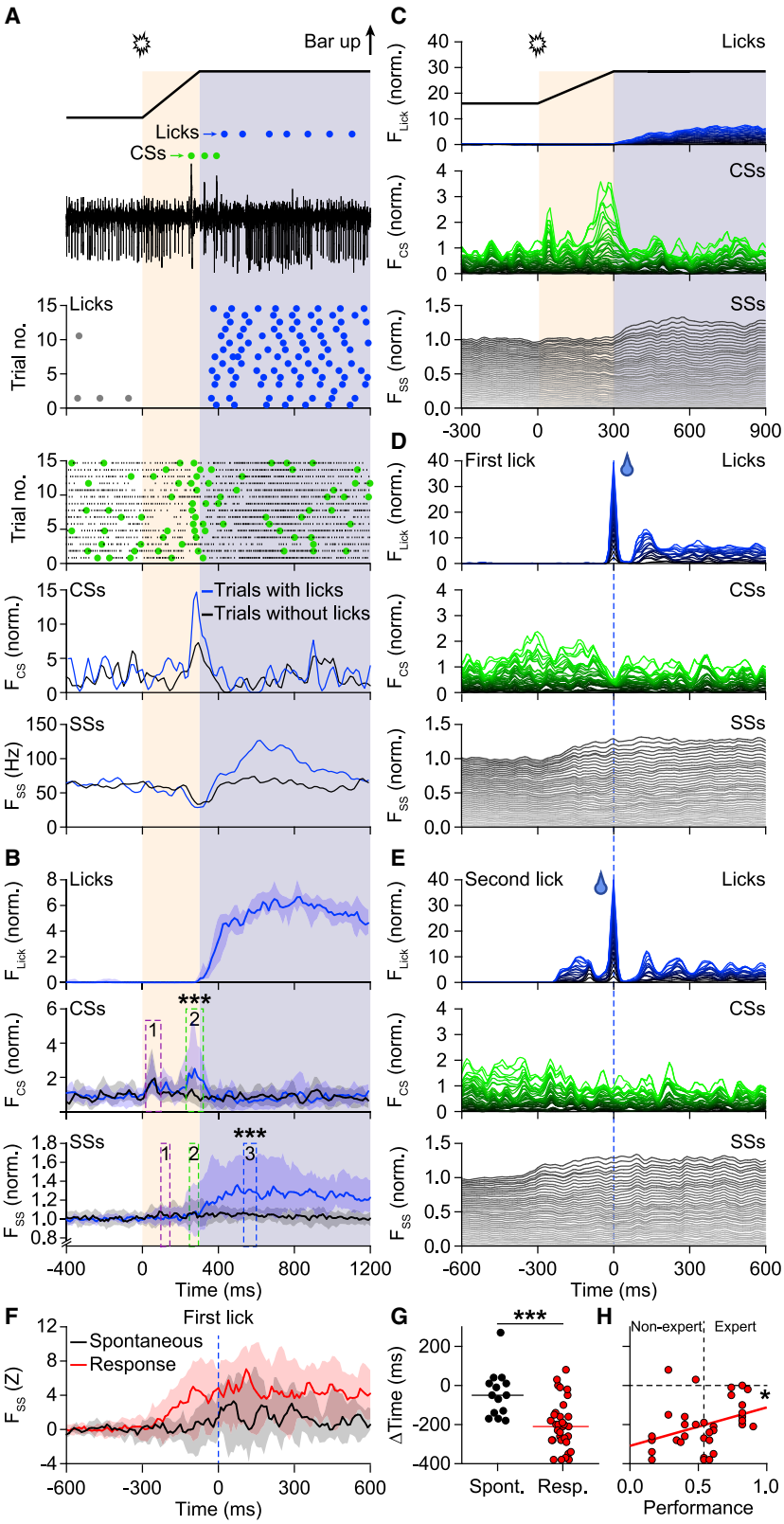

Figure 4. CSs relate more to sensory input, and SSs relate more to motor output

(A) Electrophysiological trace, scatterplots, and PSTHs during trials with (hit and FA) and without (miss and correct rejection) licking from an exemplary mouse.

(B) PSTHs of 16 mice and 42 PCs. For CS modulation, only PCs with statistically significant modulation were included (34 cells). CS modulation during the first (sound-evoked) peak was not different between trials with and without licking ($p = 0.784$, $W = -37$), but it was during the second (touch-related) peak ($p < 0.001$, $W = 437$). SS modulation was not significantly different during the no-lick period but was during the response window (values for the three intervals indicated in the graph: $p = 0.812$, $W = -39$; $p = 0.216$, $W = 199$; $p < 0.000$, $W = 577$, respectively). Medians and IQRs; Wilcoxon matched-pairs tests.

(C) Stacked line plots during hit trials aligned on trial onset. The experiments are sorted from smallest to largest modulation and scaled so that the brightest lines indicate population averages. The two CS peaks are clearly visible, as is the increase in SS firing after the onset of the response window. For this analysis, we included all recorded neurons.

(D) As in (C), but now with each trial aligned on the first lick in the response window.

(E) As in (C), but now triggered on the second lick of each trial, which was the first rewarded lick per trial. Ordering in (C)–(E) based on (C).

(F) Rewarded licking bouts in trained mice showed a stronger increase in SS firing than did unrewarded spontaneous licking bouts in untrained mice. Medians and IQRs.

(G and H) The interval between the first detected lick of licking bouts and the start of increased SS firing (first bin exceeding $Z = 3$) was larger in trained mice ($p < 0.001$, Mann-Whitney test) (G), evident also in Spearman correlation with performance ($r = 0.389$, $p = 0.025$) (H).

See also Figures S5 and S6.

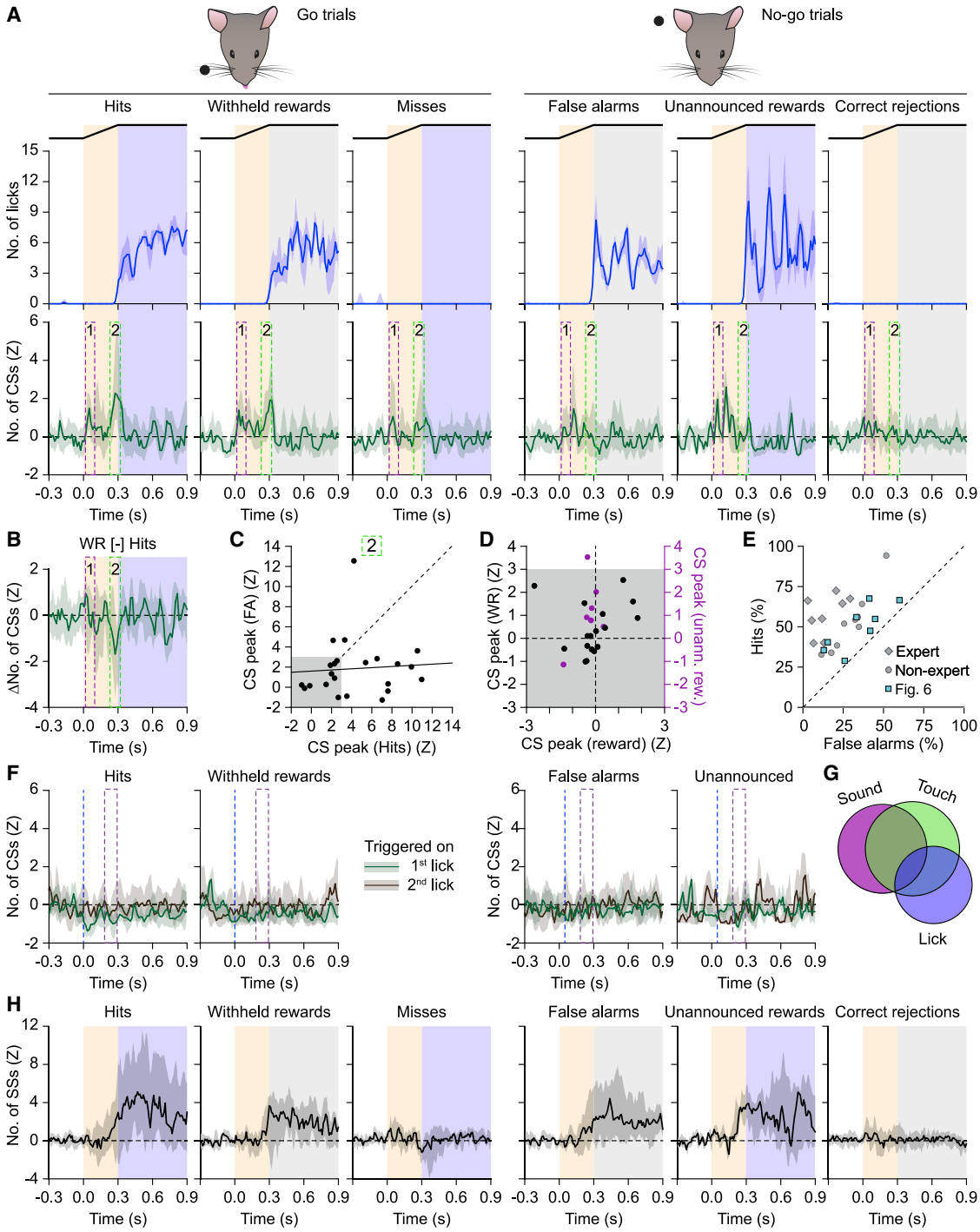

Figure 5. Withheld or unannounced rewards have little impact on PC activity in trained mice

(A) Comparisons of licking behavior and CS firing of 23 PCs in eight trained mice tested while withholding rewards in 20% of the go trials and allowing, in 20% of the no-go trials, licking during the response window to result in an unannounced reward. Time intervals 1 and 2 indicate response windows following sound and touch, respectively. Lines indicate medians, shades IQRs.

(B) Subtracted curves for withheld reward (WR) and hit trials, showing no obvious CS modulation as a result of reward omission.

(C) CS modulation evoked by whisker touch (interval 2) was stronger during hit than during FA trials, in line with the absence of touch during the latter trial type. Linear regression: r = 0.07, p = 0.746.

(D) Scatterplot showing the general absence of CS modulation during either hit trials (x axis), WRs (black), or unannounced rewards (magenta). Values are derived from the time interval shown in (F).

(legend continued on next page)

go trials nor unannounced rewards during a subset of no-go trials were experienced as salient enough to trigger CSs. However, as reward delivery did not occur at a fixed time within the trial but was triggered by the first lick during the response window, we could possibly have missed a subtle CS modulation. Hence, we subsequently aligned CS firing on the timing of the first lick, using the latency for reward-induced responses in naive mice for further analysis (Figures S3P and S3Q). In none of the trial types with licking was increased CS firing observed (Figure 5F). Thus, we conclude that reward expectation and/or delivery was not encoded by CSs in our trained mice, probably reflecting the absence of very strong expectations under these conditions. Instead, CS firing was associated with the sensory cues and licking (Figure 5G). Likewise, reward expectation and reward delivery were also not reflected in SS firing (Figure 5H).

Ca^{2+} imaging reveals bidirectional evolution of CS responses in individual cells

Our analyses so far suggested that PC activity in crus 1 and 2, and especially that of CSs, adapts during learning and relates to preparation of choice performance. Correlations between CS timing and behavioral performance differed between naive, non-expert and expert mice but were not obvious at the trial level. To further study changes in CS patterns of individual cells over consecutive days, we repeated the learning experiment in PCs carrying the genetic Ca^{2+} indicator GCaMP6f in crus 1 and imaged CS activity during learning using a miniaturized fluorescence microscope (Figures 6A–6D and S7A).

Altering CS timing during learning comprised multiple events in individual cells: decrease of the first (sound-related) and increase of the second (following touch) CS peaks occurred asynchronously. After 13 days of training, the first peak was not noticeably smaller than a week before ($p = 0.420$, $\chi^2 = -0.806$, Dunn's post hoc test after Friedman's two-way ANOVA), in contrast to the second peak ($p = 0.001$, $\chi^2 = -3.304$). Afterward, the first peak decreased significantly ($p < 0.001$, $\chi^2 = 3.465$; Figures 7E–7I). These results mirrored the behavioral changes: becoming first engaged in the task and licking more often, initially with improper timing, but gradually improving (Figure 2).

At trials with licks during the no-lick period, an aversive air puff was given to the nose, which triggered CS firing. The response to the aversive puff also disappeared during training (Figures S7B and S7C). Thus, the salience of the aversive puff for evoking CS firing seems to decrease during training, as for the sound cue, and this switch occurs at the level of individual cells.

Blocking entrainment of SS increases reduces learning efficacy of choice performance

The pattern of CS and SS activity shifts over time during training, which may facilitate decision-making. SS increases appear to consistently follow those of CSs, and we wondered to what extent they were causally related. Hence, we studied *Pcp2-Pppr3r1* knockout (KO) mice (Figure 7A), which are deficient in postsynaptic long-term potentiation (LTP) at the PF-PC inputs, while leaving CS activity intact (Schonewille et al., 2010). *Pcp2-Pppr3r1* KO mice required significantly more time to master the task than did wild-type (WT) littermates (fraction correct trials: $p = 0.006$, $F = 3.215$, df = 17, interaction effect, repeated-measures ANOVA with Greenhouse-Geisser correction; Figure 7B). Even so, *Pcp2-Pppr3r1* KO mice were eventually able to execute timed licking (Figures 7C and S8B). CS activity in crus 1 and 2 of *Pcp2-Pppr3r1* KO mice appeared unaffected during spontaneous behavior, whereas the SS activity was reduced and more regular (Figure S8A), the latter in agreement with previous findings (Rahmati et al., 2014; Romano et al., 2018; Schonewille et al., 2010). Likewise, when we analyzed CS activity during hit trials, we did not observe significant differences. The amplitudes of neither the first nor the second peak were significantly different between *Pcp2-Pppr3r1* WT and KO mice ($p = 0.462$, $U = 58.5$ and $p = 0.388$, $U = 56$, respectively, Mann-Whitney tests; Figure 7D). In contrast, the SS pattern was completely altered in *Pcp2-Pppr3r1* KO mice: rather than a broad increase in SS firing during the response window, trained *Pcp2-Pppr3r1* KO mice showed a decrease in SS firing (e.g., during 545–605 ms: $p < 0.001$, $U = 58$, Mann-Whitney test; Figure 7E). Thus, mutant mice deficient in PC LTP fail to show an upregulation of SS firing during learning. This effect appeared to be specific for the response stage because SS firing during the early (non-response) phase of the trial was equally low in trained WT and *Pcp2-Pppr3r1* KO mice (95–145 ms: $p = 0.826$, $U = 18.5$, Mann-Whitney test; Figure 7E). Alignment of spiking activity on the first lick demonstrated that during licking, both CS and SS firing was reduced in *Pcp2-Pppr3r1* KO mice (Figures S8B–S8D).

To find out whether this behavioral phenotype is specific for LTP-deficient mice, we subjected long-term depression (LTD)-deficient *Gria2*-Δ7 knock-in (KI) mice (Schonewille et al., 2011) to the same task. Despite the absence of LTD, we did not observe any evidence of impaired learning (Figure S8E). Together, our findings suggest that the potentiation-mediated changes in SS activity that follow changes in CS activity contribute to choice performance but are not required for the ability to lick.

DISCUSSION

To optimize movements in any given context, our brain continuously makes predictions about the outcomes of our actions. The olivocerebellar system plays a critical role in creating such expectations and in adapting movements on the basis of sensory feedback (Heffley et al., 2018; Hull, 2020; Kostadinov et al., 2019; Larry et al., 2019; Moberget and Ivry, 2019; Tsutsumi

(E) Scatterplot visualizing the discrimination between go and no-go trials for each mouse: the farther above the 45° line, the better the performance. The gray symbols (diamond, experts; circles, non-experts) refer to the mice tested on the normal paradigm without withheld and unannounced rewards (Figure 3E).
(F) CS modulation aligned on the first licks (that triggered the reward in hit and unexpected reward trials) in green, with alignment on second lick in gray. The time interval (magenta rectangle) captures the response to reward in naive mice (see Figures S3P and S3Q).
(G) Venn diagram demonstrating the overlap in statistically significant CS modulation among sound-, touch-, and lick-triggered CS modulation at the level of individual PCs.
(H) SS modulation related largely to the time course of licking.

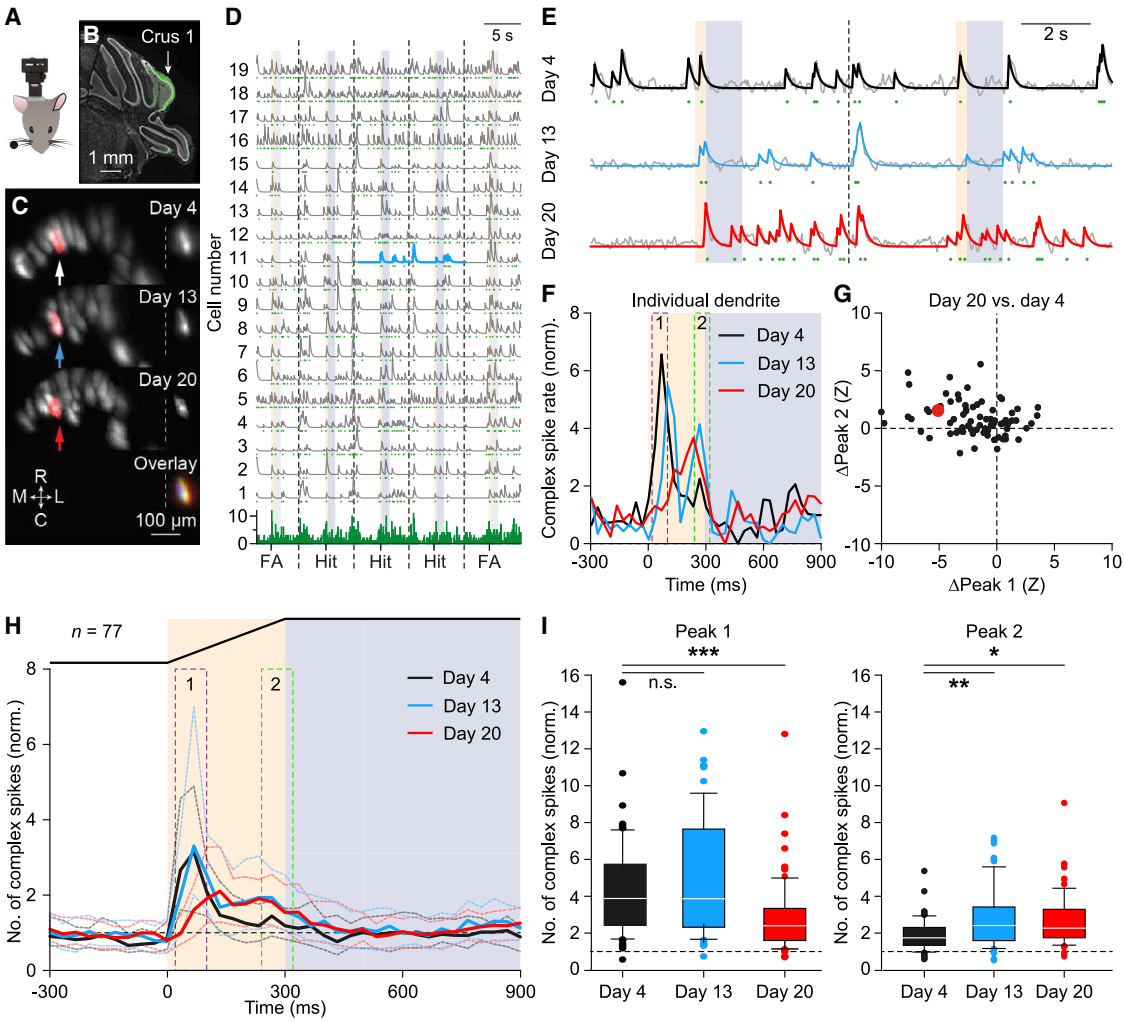

Figure 6. CS plasticity occurs asynchronously

(A) In four mice, we performed fluorescent imaging using a miniscope to monitor PC Ca^{2+} transients during training.

(B) Post-mortem histological analysis confirmed GCaMP6f expression in crus 1. Scale bar: 1 mm.

(C) Field of view with 19 dendrites of the same mouse at the fourth, thirteenth, and twentieth days of training. The consistent location of the dendrite marked in red is shown in the overlay (bottom). Scale bar: 100 µm.

(D) Representative recording on training day 13. The bottom row shows the number of dendrites active at any frame. The light blue fragment is enlarged in (E) and concerns the dendrite highlighted in (C).

(E) Fluorescent transients of an individual dendrite at days 4, 13, and 20. The gray lines represent unfiltered and the colored lines convoluted traces. The green symbols in (D) and (E) indicate identified fluorescent transients caused by CS firing.

(F) PSTHs of the CSs of the dendrite illustrated in (E). Note that the first (sound-evoked) peak changed only during the second half of the training, while the second (touch-induced) peak emerged during the first half.

(G) Scatterplot of the changes in the amplitudes of the first (sound-evoked) and second (touch-induced) CS peaks in 77 dendrites that could be identified throughout training. Plotted are the differences between day 20 and day 4. The example dendrite is indicated in red.

(H) Median histograms of all 77 dendrites from four mice that could be followed throughout training. Dotted lines indicate IQRs.

(I) Boxplots showing the CS peaks during the first (15–115 ms) and the second (215–315 ms) peaks. Colored area = 25%–75% confidence interval, with the medians indicated. Whiskers show 10%–90% confidence interval, with outliers as individual data points. First peak: Friedman's two-way ANOVA ($p < 0.001$, $\chi^2 = 20.597$, $n = 77$, $df = 2$) with Dunn's post hoc test (days 4–13: $p = 0.420$, $\chi^2 = -0.806$; days 4–20: $p < 0.001$, $\chi^2 = 3.465$). Second peak: Friedman's two-way ANOVA ($p = 0.003$, $\chi^2 = 11.403$, $n = 77$, $df = 2$) with Dunn's post hoc test (days 4–13: $p = 0.001$, $\chi^2 = -3.304$; days 4–20: $p = 0.024$, $\chi^2 = -2.256$; both significant after Bonferroni correction).

See also Figure S7.

et al., 2019; Brooks et al., 2015; Cayco-Gajic and Silver, 2019; Tzvi et al., 2020; Wolpert et al., 1998). Cerebellar control of sensorimotor learning has been particularly well studied in reflex adaptation (Koekkoek et al., 2003; Ohmae and Medina, 2015; Steinmetz et al., 1987; ten Brinke et al., 2015; Halverson et al., 2015; Boele et al., 2018), but it expands beyond the domain

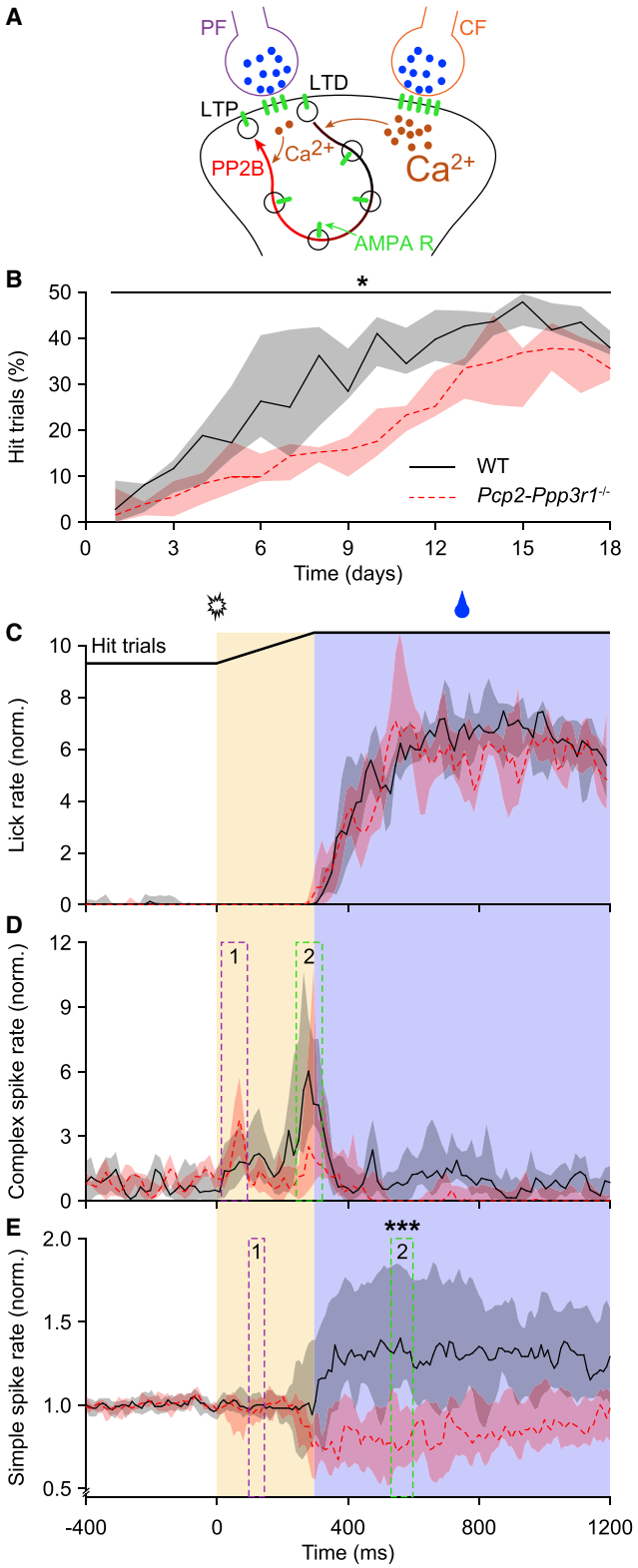

Figure 7. Impairment of PC LTP reduced learning efficacy, but not motor performance, in trained mice

(A) *Pcp2-Ppp3r1* KO mice lack protein phosphatase 2B (PP2B) specifically in their PCs. As a consequence, the KO mice do not express parallel fiber (PF)-PC LTP. Co-activation of PFs and the climbing fiber (CF) leads to a large influx of Ca^{2+} into PCs, favoring PF-PC LTD, while activation of PFs in the absence of CF activity induces LTP, involving activation of PP2B in WT mice. Schematic drawing adapted with permission from Romano et al. (2018).

(B) During training, *Pcp2-Ppp3r1* KO mice took longer to learn to time their licks than did their WT controls. Medians (shades: IQR) of the fraction of hit trials in nine KO and nine WT mice.

(C–E) PSTHs (medians with IQR) of the number of licks (C), CSs (D), and SSs (E) during hit trials of WT and mutant mice. The CSs were taken only from significantly responsive cells (9 in KO and 16 in WT mice after completion of training) and SSs from all 14 and 27 cells, respectively. Although actual motor performance was comparable, SS modulation was different (95–145 ms: $p = 0.826$, $W = 180.5$; 545–605 ms: $p < 0.001$, $U = 58$, Mann-Whitney tests of KO versus WT cells).

See also Figure S8.

of classical forms of conditioning and can, for instance, also underlie reward prediction (Heffley and Hull, 2019; Heffley et al., 2018; Hull, 2020; Kostadinov et al., 2019; Larry et al., 2019; Tsutsumi et al., 2019). Here, we demonstrate that the olivocerebellar system is also involved in learning a complex form of decision-making based on sensory discrimination, and it does so by changing responses of PCs from one modality (in this case, sound) to another (in this case, touch). Indeed, because of a change in the salience of sensory inputs, both CS and SS modulations of PCs adapt, with their prime impact on the readiness to act and output performance, respectively.

Learning a complex sensory discrimination task

Whisker-based discrimination tasks were initially designed for rats (Mehta et al., 2007) and later were adapted for mice (O'Connor et al., 2010). Since then, many variants have been developed (Huber et al., 2012; Xu et al., 2012; Rahmati et al., 2014; Hong et al., 2018), including using visual cues (Groblewski et al., 2020) or left-right choice paradigms (Gao et al., 2018; Guo et al., 2014; Li et al., 2015). In the variation of the go/no-go paradigm used in this study, mice first engaged in licking upon perception of the sound cue, subsequently postponed the reaction by waiting for the tactile cue, and finally stopped engaging in no-go trials. Similar to left-right choice paradigms, our go/no-go discrimination paradigm took 2–3 weeks to learn and is likely to also rely on neocortical activity to make decisions (Gao et al., 2018; Guo et al., 2014; Li et al., 2015; O'Connor et al., 2010; Inagaki et al., 2018). This stands in marked contrast to learning to associate the paired presentation of a particular sensory stimulus and a reward, which is easier and can be mastered within 1–2 days (Heffley and Hull, 2019; Heffley et al., 2018; Kostadinov et al., 2019; Larry et al., 2019).

Limitations of the study

Most mice had difficulty completely mastering the sensory discrimination task and kept making mistakes. While these mistakes helped us to differentiate between different aspects of task performance, they also obfuscated the degree to which mice could predict reward delivery. On top of this, the level of motivation may affect responses, which is a common aspect of go/no-go tasks (Martinelli et al., 2017; Liddle et al., 2011; O'Connor et al., 2010). We mitigated the impact of motivation by disregarding the later parts of the sessions, when mice failed to participate during at least 10 consecutive trials.

CSs encode sensory salience, engaging a readiness to act

Although most PCs show CS responses to broad classes of sensory input, they have their individual preferences for certain inputs over others (Ju et al., 2019; Apps and Garwicz, 2005; Bosman et al., 2010). Our current data highlight that sensory encoding by CSs is a dynamic process that adapts to salience, which may relate to selective attention. In untrained mice (i.e., mice accustomed to licking in the recording setup, but not previously subjected to the stimulation device), the sound cue triggered considerably fewer CSs than in naive mice that did not lick (cf. Figures 3 and S3); water rewards apparently deviated the attention from sound. Accordingly, in trained mice, the ability to suppress sound-related CSs correlated with preparation of choice performance. Furthermore, once mice became experts, their CS response to sound was virtually nihilated, but that to the relatively subtle tactile cue was strengthened. Remarkably, in a minority of PCs, CSs following the timing of touch during go trials were prominent during no-go trials (Figure 3C), despite the absence of touch during the latter. Furthermore, water rewards triggered CSs in untrained, but not in trained, mice. Apparently, expert mice were expecting rewards at specific moments and were not surprised by their actual appearance. Deviating from the normal rules and rewarding licks during no-go trials also was not salient enough to trigger CSs in trained mice. Finally, the aversive puff given upon licking in the no-lick period gradually lost its ability to trigger CSs during training. Thus, CSs in crus 1 and 2 may encode sound, whisker touch, or reward, but they are not reliable detectors for any of them, and the responses depend on the context.

Longitudinal imaging experiments of CS activity of individual PCs demonstrated that during different stages of learning, distinct inputs could elicit CS responses in the same cells. These data indicate that the adaptive changes in the salience of inputs originate upstream of PCs. As the IO, from where the CFs originate, comprises a mixture of ascending excitatory inputs from sensory sources, descending excitatory inputs from cerebral cortical activity mediated via the mesodiencephalic junction, and inhibitory feedback from the cerebellar or vestibular nuclei (Bosman et al., 2011; Wang et al., 2021) (Figure 1A), it will be interesting to study this reconfiguration.

Similar adaptive changes in the salience of inputs that elicit CSs have been detected during eyeblink conditioning (Ohmae and Medina, 2015; ten Brinke et al., 2015). Yet, whereas in eyeblink conditioning the perception of salience and readiness to act are moving toward the conditioned stimulus (i.e., the CS signals are accelerated within the interstimulus interval), in our discrimination task, they are moving in the opposite direction (i.e., they are decelerated within the trials). The common mechanism during both forms of learning may be that the CF signals move in time toward the most salient sensory input that needs to engage a readiness to act, be it to prepare for closing the eyelid or making a proper choice. Unless synchronously involved in triggering a crude reflex following an unexpected perturbation of an ongoing movement (Van Der Giessen et al., 2008; De Gruijl et al., 2014; Hoogland et al., 2015), CSs appear relatively ill-suited for ongoing fine motor control following learning due to their low frequency, their resistance against frequency modulation, and the large jitter in their timing (De Zeeuw et al., 2011; Negrello et al., 2019; Albus, 1971; Marr, 1969). Thus, the CSs in our demanding discrimination task adapt to the subjective salience and set the stage for the behavioral response, referred to as readiness to act, but do not directly control the precise timing of actual motor responses.

SS increases facilitate choice performance

Whereas SSs started to increase only at the onset of spontaneous licking, during the discrimination task, they occurred earlier, closely adhering to the period when the choices were made. In contrast to CSs, SSs were associated more closely to the motor activity than to the sensory stimulation. In *Pcp2-Ppr3r1* KO mice, which are defect in the induction of PC-specific LTP, we found that this increase in SS firing did not occur, in line with previous findings (Rahmati et al., 2014). Unlike LTD-deficient mice, it took the LTP-deficient mice significantly longer to reach the same level of choice performance. The finding that the LTP-deficient mice ultimately, after more days of training, still reached the same performance level as WTs suggests that *Pcp2-Ppr3r1* KO mice followed an alternative, less efficient learning strategy. This is reminiscent of skill development in humans born without a cerebellum, who show severely delayed motor development but can eventually reach relatively normal levels of motor control (Tavano et al., 2007; Boyd, 2010; Yu et al., 2015). Likewise, in *Pcp2-PKCi* mice adaptation, the vestibulo-ocular reflex is delayed but not completely ablated (van Alphen and De Zeeuw, 2002). In other words, in the chronic absence of a cerebellum, or of a plasticity mechanism mediating changes in SS activity in PCs, learning is less efficient, but still possible, as mechanisms of developmental compensation can occur. In this respect, it is important to note that we also observed a significant deficit in choice performance when we corrupted the SSs activity of PCs in crus 1 and 2 acutely, applying optogenetic stimulation at the proper window of the discrimination task. Hence, choice performance was affected following not only chronic, but also acute, manipulation of SS activity.

Since SS modulation occurs during licking (Bryant et al., 2010), it may also be related to movement initiation (Dacre et al., 2021). However, aberrant relations between SS firing and licking in *Pcp2-Ppr3r1* KO mice calls into question to what extent these are directly causally linked in our paradigm. Instead, the well-timed increase in SS firing may help to make the correct choice and only subsequently facilitate the correct motor response.

CS-SS modulations

Most SSs occurred after the CS response to the sound cue in naive mice and after the CS response to the tactile cue in trained mice. Our data reveal a heterogeneity in CS firing, but the majority of recorded PCs show learning-dependent changes in CS firing, with different firing patterns during go and no-go trials in trained mice. These data are in line with the possibility that the SSs are at the highest level when the CS responses are low, in the period directly after the preceding CS (Badura et al., 2013; De Zeeuw, 2021; Herzfeld et al., 2018; ten Brinke et al., 2015; Yang and Lisberger, 2014). Moreover, they are also compatible with the plasticity rule that a decrease in CF activity induces

LTP at the PF to PC input (Coesmans et al., 2004; Gao et al., 2012; Romano et al., 2018) as well as LTD at the PF to molecular layer interneuron input, together facilitating SS output (Gaffield and Christie, 2017). Thus, a change in the salience of the sensory input that evokes a CS response may well affect the moment of occurrence of the SS response via a change in potentiation of PCs.

The consistent and conjunctive shifts of CS and SS activities across our operant learning paradigm are reminiscent of other examples that have been observed during motor adaptation. When a monkey makes a saccade toward a target but fails to reach that target, CS firing encodes the motor error and presumably triggers synaptic plasticity to alter SS firing during the next trial (Herzfeld et al., 2018; Yang and Lisberger, 2014). Similarly, when the direction of CS modulation during compensatory eye movements is reversed due to a rerouting of the contralateral CFs toward the ipsilateral side, the direction of SS modulation also reverses, even when the laterality of the mossy fibers remains intact (Badura et al., 2013). Hence, during various forms of motor learning, CSs can direct the plasticity of PF to PC synapses and thereby suppress or promote SS firing (Coesmans et al., 2004; Ito, 2002b; Ohtsuki et al., 2009; Romano et al., 2018; Yang and Lisberger, 2014). The current study suggests that the plasticity rules implicated in motor learning probably also hold, at least to some extent, for non-motor aspects of cerebellar learning.

Conclusions

CFs projecting to crus 1 and 2 encode sensory input in a context-dependent manner and adapt their responsiveness during learning. Sensory stimuli that are perceived as salient for a given context, and that are associated with anticipated behavioral responses, are more prone to activate CFs. When a particular sensory input signaled by a CF is replaced by another more salient stimulus, its timing shifts toward the moment when readiness to act is advantageous. Reflecting different stages of learning, the resulting CS pattern presumably guides plasticity in PCs, concomitantly shifting the timing of SSs (De Zeeuw, 2021). SS activity, in turn, facilitates choice performance and related motor output. Thus, we hypothesize that during discrimination learning, CFs signal the salience of inputs, engaging a readiness to act, which, in turn, is established by SS output, thereby improving choice performance and motor output.

STAR★METHODS

Detailed methods are provided in the online version of this paper and include the following:

- KEY RESOURCES TABLE
- RESOURCE AVAILABILITY
  - Lead contact
  - Materials availability
  - Data and code availability
- EXPERIMENTAL MODEL AND SUBJECT DETAILS
- METHOD DETAILS
  - Habituation and water restriction
  - Behavioral paradigm and surgical procedures
  - Optogenetic stimulation
  - Electrophysiology
  - Behavioral data analysis
  - Electrophysiological data analysis
  - Miniscope imaging
  - Extraction and analysis of calcium transients
  - Whisker movement tracking
- QUANTIFICATION AND STATISTICAL ANALYSIS

SUPPLEMENTAL INFORMATION

Supplemental information can be found online at https://doi.org/10.1016/j.celrep.2021.110116.

ACKNOWLEDGMENTS

The authors wish to thank Sander van Gurp, Sander Lindeman, and Mario Negrello for their contributions to the pilot phase of this project; Hugo Hoedemaker, Maryam El Hamdioui, Danique Broere, Morgann Dettingmeijer, and Celia Mak for their aid with surgeries and data collection; Marcel van der Heijden for recording and analyzing the sound of the stimulator; Sanne Smid for help with video analysis; and Gerard Borst and Steven Kushner for discussions on the interpretation and presentation of the results. Financial support was provided by the Netherlands Organization for Scientific Research (NWO-ALW; C.I.D.Z.), the Dutch Organization for Medical Sciences (ZonMW; C.I.D.Z.), BIG (C.I.D.Z.), Medical Neuro-Delta (C.I.D.Z.), INTENSE LSH-NWO (C.I.D.Z.), ERC-adv and ERC-POC (C.I.D.Z.), Van Raamsdonk-fonds (C.I.D.Z.), 3V-Fonds KNAW (T.M.H. and C.I.D.Z.), Albinism Fonds NIN (C.I.D.Z.), and Health Holland (TKI-LSH LSHM18001 [T.M.H.] and TKI-LSH EMCLSH21017 [L.W.J.B.]).

AUTHOR CONTRIBUTIONS

Conceptualization, L.B., L.W.J.B., and C.I.D.Z.; methodology, L.B., T.M.H., and L.W.J.B.; software, L.B., T.M.H., and L.W.J.B.; validation, L.B., T.M.H., and L.W.J.B.; formal analysis, L.B.; investigation, L.B. and V.R.; resources, T.M.H. and L.W.J.B.; data curation, L.B.; writing – original draft, L.B. and L.W.J.B.; writing – review & editing, T.M.H., L.W.J.B., and C.I.D.Z.; visualization, L.B., T.M.H., and L.W.J.B.; supervision, L.W.J.B. and C.I.D.Z.; project administration, L.B. and L.W.J.B.; funding acquisition, T.M.H., L.W.J.B., and C.I.D.Z.

DECLARATION OF INTERESTS

The authors declare no competing interests.

INCLUSION AND DIVERSITY

We worked to ensure sex balance in the selection of non-human subjects.

Received: September 16, 2020
Revised: July 6, 2021
Accepted: November 19, 2021
Published: December 14, 2021

REFERENCES

Abdelgabar, A.R., Suttrup, J., Broersen, R., Bhandari, R., Picard, S., Keysers, C., De Zeeuw, C.I., and Gazzola, V. (2019). Action perception recruits the cerebellum and is impaired in patients with spinocerebellar ataxia. Brain *142*, 3791–3805.

Albus, J.S. (1971). Theory of cerebellar function. Math. Biosci. *10*, 25–61.

Allen, G., Buxton, R.B., Wong, E.C., and Courchesne, E. (1997). Attentional activation of the cerebellum independent of motor involvement. Science *275*, 1940–1943.

Apps, R., and Garwicz, M. (2005). Anatomical and physiological foundations of cerebellar information processing. Nat. Rev. Neurosci. *6*, 297–311.

Badura, A., Schonewille, M., Voges, K., Galliano, E., Renier, N., Gao, Z., Witter, L., Hoebeek, F.E., Chédotal, A., and De Zeeuw, C.I. (2013). Climbing fiber input shapes reciprocity of Purkinje cell firing. Neuron *78*, 700–713.

Barski, J.J., Dethleffsen, K., and Meyer, M. (2000). Cre recombinase expression in cerebellar Purkinje cells. Genesis *28*, 93–98.

Boele, H.J., Peter, S., Ten Brinke, M.M., Verdonschot, L., IJpelaar, A.C.H., Rizopoulos, D., Gao, Z., Koekkoek, S.K.E., and De Zeeuw, C.I. (2018). Impact of parallel fiber to Purkinje cell long-term depression is unmasked in absence of inhibitory input. Sci. Adv. *4*, eaas9426.

Bosman, L.W.J., Koekkoek, S.K.E., Shapiro, J., Rijken, B.F.M., Zandstra, F., van der Ende, B., Owens, C.B., Potters, J.W., de Gruijl, J.R., Ruigrok, T.J.H., and De Zeeuw, C.I. (2010). Encoding of whisker input by cerebellar Purkinje cells. J. Physiol. *588*, 3757–3783.

Bosman, L.W.J., Houweling, A.R., Owens, C.B., Tanke, N., Shevchouk, O.T., Rahmati, N., Teunissen, W.H.T., Ju, C., Gong, W., Koekkoek, S.K.E., and De Zeeuw, C.I. (2011). Anatomical pathways involved in generating and sensing rhythmic whisker movements. Front. Integr. Nuerosci. *5*, 53.

Boyd, C.A.R. (2010). Cerebellar agenesis revisited. Brain *133*, 941–944.

Brissenden, J.A., Tobyne, S.M., Osher, D.E., Levin, E.J., Halko, M.A., and Somers, D.C. (2018). Topographic cortico-cerebellar networks revealed by visual attention and working memory. Curr. Biol. *28*, 3364–3372.e5.

Brooks, J.X., Carriot, J., and Cullen, K.E. (2015). Learning to expect the unexpected: rapid updating in primate cerebellum during voluntary self-motion. Nat. Neurosci. *18*, 1310–1317.

Bryant, J.L., Boughter, J.D., Gong, S., LeDoux, M.S., and Heck, D.H. (2010). Cerebellar cortical output encodes temporal aspects of rhythmic licking movements and is necessary for normal licking frequency. Eur. J. Neurosci. *32*, 41–52.

Buschman, T.J., and Kastner, S. (2015). From behavior to neural dynamics: An integrated theory of attention. Neuron *88*, 127–144.

Cayco-Gajic, N.A., and Silver, R.A. (2019). Re-evaluating circuit mechanisms underlying pattern separation. Neuron *101*, 584–602.

Coesmans, M., Weber, J.T., De Zeeuw, C.I., and Hansel, C. (2004). Bidirectional parallel fiber plasticity in the cerebellum under climbing fiber control. Neuron *44*, 691–700.

Dacre, J., Colligan, M., Clarke, T., Ammer, J.J., Schiemann, J., Chamosa-Pino, V., Claudi, F., Harston, J.A., Eleftheriou, C., Pakan, J.M.P., et al. (2021). A cerebellar-thalamocortical pathway drives behavioral context-dependent movement initiation. Neuron *109*, 2326–2338.e8.

de Groot, A., van den Boom, B.J.G., van Genderen, R.M., Coppens, J., van Veldhuijzen, J., Bos, J., Hoedemaker, H., Negrello, M., Willuhn, I., De Zeeuw, C.I., and Hoogland, T.M. (2020). NINscope, a versatile miniscope for multi-region circuit investigations. eLife *9*, e49987.

De Gruijl, J.R., Hoogland, T.M., and De Zeeuw, C.I. (2014). Behavioral correlates of complex spike synchrony in cerebellar microzones. J. Neurosci. *34*, 8937–8947.

De Zeeuw, C.I. (2021). Bidirectional learning in upbound and downbound microzones of the cerebellum. Nat. Rev. Neurosci. *22*, 92–110.

De Zeeuw, C.I., Hoebeek, F.E., Bosman, L.W.J., Schonewille, M., Witter, L., and Koekkoek, S.K. (2011). Spatiotemporal firing patterns in the cerebellum. Nat. Rev. Neurosci. *12*, 327–344.

Gaffield, M.A., and Christie, J.M. (2017). Movement rate is encoded and influenced by widespread, coherent activity of cerebellar molecular layer interneurons. J. Neurosci. *37*, 4751–4765.

Gao, Z., van Beugen, B.J., and De Zeeuw, C.I. (2012). Distributed synergistic plasticity and cerebellar learning. Nat. Rev. Neurosci. *13*, 619–635.

Gao, Z., Davis, C., Thomas, A.M., Economo, M.N., Abrego, A.M., Svoboda, K., De Zeeuw, C.I., and Li, N. (2018). A cortico-cerebellar loop for motor planning. Nature *563*, 113–116.

Groblewski, P.A., Ollerenshaw, D.R., Kiggins, J.T., Garrett, M.E., Mochizuki, C., Casal, L., Cross, S., Mace, K., Swapp, J., Manavi, S., et al. (2020). Characterization of learning, motivation, and visual perception in five transgenic mouse lines expressing GCaMP in distinct cell populations. Front. Behav. Neurosci. *14*, 104.

Guo, Z.V., Li, N., Huber, D., Ophir, E., Gutnisky, D., Ting, J.T., Feng, G., and Svoboda, K. (2014). Flow of cortical activity underlying a tactile decision in mice. Neuron *81*, 179–194.

Halverson, H.E., Khilkevich, A., and Mauk, M.D. (2015). Relating cerebellar purkinje cell activity to the timing and amplitude of conditioned eyelid responses. J. Neurosci. *35*, 7813–7832.

Heffley, W., and Hull, C. (2019). Classical conditioning drives learned reward prediction signals in climbing fibers across the lateral cerebellum. eLife *8*, e46764.

Heffley, W., Song, E.Y., Xu, Z., Taylor, B.N., Hughes, M.A., McKinney, A., Joshua, M., and Hull, C. (2018). Coordinated cerebellar climbing fiber activity signals learned sensorimotor predictions. Nat. Neurosci. *21*, 1431–1441.

Helmuth, L.L., Ivry, R.B., and Shimizu, N. (1997). Preserved performance by cerebellar patients on tests of word generation, discrimination learning, and attention. Learn. Mem. *3*, 456–474.

Herzfeld, D.J., Kojima, Y., Soetedjo, R., and Shadmehr, R. (2018). Encoding of error and learning to correct that error by the Purkinje cells of the cerebellum. Nat. Neurosci. *21*, 736–743.

Hong, Y.K., Lacefield, C.O., Rodgers, C.C., and Bruno, R.M. (2018). Sensation, movement and learning in the absence of barrel cortex. Nature *561*, 542–546.

Hoogland, T.M., De Gruijl, J.R., Witter, L., Canto, C.B., and De Zeeuw, C.I. (2015). Role of synchronous activation of cerebellar Purkinje cell ensembles in multi-joint movement control. Curr. Biol. *25*, 1157–1165.

Huber, D., Gutnisky, D.A., Peron, S., O'Connor, D.H., Wiegert, J.S., Tian, L., Oertner, T.G., Looger, L.L., and Svoboda, K. (2012). Multiple dynamic representations in the motor cortex during sensorimotor learning. Nature *484*, 473–478.

Hull, C. (2020). Prediction signals in the cerebellum: beyond supervised motor learning. eLife *9*, e54073.

Inagaki, H.K., Inagaki, M., Romani, S., and Svoboda, K. (2018). Low-dimensional and monotonic preparatory activity in mouse anterior lateral motor cortex. J. Neurosci. *38*, 4163–4185.

Ito, M. (2002a). Historical review of the significance of the cerebellum and the role of Purkinje cells in motor learning. Ann. N Y Acad. Sci. *978*, 273–288.

Ito, M. (2002b). The molecular organization of cerebellar long-term depression. Nat. Rev. Neurosci. *3*, 896–902.

Ju, C., Bosman, L.W.J., Hoogland, T.M., Velauthapillai, A., Murugesan, P., Warnaar, P., van Genderen, R.M., Negrello, M., and De Zeeuw, C.I. (2019). Neurons of the inferior olive respond to broad classes of sensory input while subject to homeostatic control. J. Physiol. *597*, 2483–2514.

Knudsen, E.I. (2018). Neural circuits that mediate selective attention: A comparative perspective. Trends Neurosci. *41*, 789–805.

Koekkoek, S.K.E., Hulscher, H.C., Dortland, B.R., Hensbroek, R.A., Elgersma, Y., Ruigrok, T.J.H., and De Zeeuw, C.I. (2003). Cerebellar LTD and learning-dependent timing of conditioned eyelid responses. Science *301*, 1736–1739.

Kostadinov, D., Beau, M., Blanco-Pozo, M., and Häusser, M. (2019). Predictive and reactive reward signals conveyed by climbing fiber inputs to cerebellar Purkinje cells. Nat. Neurosci. *22*, 950–962.

Kuhn, B., Ozden, I., Lampi, Y., Hasan, M.T., and Wang, S.S.H. (2012). An amplified promoter system for targeted expression of calcium indicator proteins in the cerebellar cortex. Front. Neural Circuits *6*, 49.

Larry, N., Yarkoni, M., Lixenberg, A., and Joshua, M. (2019). Cerebellar climbing fibers encode expected reward size. eLife *8*, e46870.

Le, T.H., Pardo, J.V., and Hu, X. (1998). 4 T-fMRI study of nonspatial shifting of selective attention: cerebellar and parietal contributions. J. Neurophysiol. *79*, 1535–1548.

Li, N., Chen, T.W., Guo, Z.V., Gerfen, C.R., and Svoboda, K. (2015). A motor cortex circuit for motor planning and movement. Nature *519*, 51–56.

Liddle, E.B., Hollis, C., Batty, M.J., Groom, M.J., Totman, J.J., Liotti, M., Scerif, G., and Liddle, P.F. (2011). Task-related default mode network modulation and inhibitory control in ADHD: effects of motivation and methylphenidate. J. Child Psychol. Psychiatry *52*, 761–771.

Lindeman, S., Hong, S., Kros, L., Mejias, J.F., Romano, V., Oostenveld, R., Negrello, M., Bosman, L.W.J., and De Zeeuw, C.I. (2021). Cerebellar Purkinje cells can differentially modulate coherence between sensory and motor cortex depending on region and behavior. Proc. Natl. Acad. Sci. USA *118*, e2015292118.

Marr, D. (1969). A theory of cerebellar cortex. J. Physiol. *202*, 437–470.

Martinelli, M.K., Mostofsky, S.H., and Rosch, K.S. (2017). Investigating the impact of cognitive load and motivation on response control in relation to delay discounting in children with ADHD. J. Abnorm. Child Psychol. *45*, 1339–1353.

Mehta, S.B., Whitmer, D., Figueroa, R., Williams, B.A., and Kleinfeld, D. (2007). Active spatial perception in the vibrissa scanning sensorimotor system. PLoS Biol. *5*, e15.

Moberget, T., and Ivry, R.B. (2019). Prediction, psychosis, and the cerebellum. Biol. Psychiatry Cogn. Neurosci. Neuroimaging *4*, 820–831.

Negrello, M., Warnaar, P., Romano, V., Owens, C.B., Lindeman, S., Iavarone, E., Spanke, J.K., Bosman, L.W.J., and De Zeeuw, C.I. (2019). Quasiperiodic rhythms of the inferior olive. PLoS Comput. Biol. *15*, e1006475.

O'Connor, D.H., Clack, N.G., Huber, D., Komiyama, T., Myers, E.W., and Svoboda, K. (2010). Vibrissa-based object localization in head-fixed mice. J. Neurosci. *30*, 1947–1967.

Ohmae, S., and Medina, J.F. (2015). Climbing fibers encode a temporal-difference prediction error during cerebellar learning in mice. Nat. Neurosci. *18*, 1798–1803.

Ohtsuki, G., Piochon, C., and Hansel, C. (2009). Climbing fiber signaling and cerebellar gain control. Front. Cell. Neurosci. *3*, 4.

Perkon, I., Kosir, A., Itskov, P.M., Tasic, J., and Diamond, M.E. (2011). Unsupervised quantification of whisking and head movement in freely moving rodents. J. Neurophysiol. *105*, 1950–1962.

Pnevmatikakis, E.A., and Giovannucci, A. (2017). NoRMCorre: An online algorithm for piecewise rigid motion correction of calcium imaging data. J. Neurosci. Methods *291*, 83–94.

Rahmati, N., Owens, C.B., Bosman, L.W.J., Spanke, J.K., Lindeman, S., Gong, W., Potters, J.W., Romano, V., Voges, K., Moscato, L., et al. (2014). Cerebellar potentiation and learning a whisker-based object localization task with a time response window. J. Neurosci. *34*, 1949–1962.

Romano, V., De Propris, L., Bosman, L.W.J., Warnaar, P., Ten Brinke, M.M., Lindeman, S., Ju, C., Velauthapillai, A., Spanke, J.K., Middendorp Guerra, E., et al. (2018). Potentiation of cerebellar Purkinje cells facilitates whisker reflex adaptation through increased simple spike activity. eLife *7*, e38852.

Romano, V., Reddington, A.L., Cazzanelli, S., Mazza, R., Ma, Y., Strydis, C., Negrello, M., Bosman, L.W.J., and De Zeeuw, C.I. (2020). Functional convergence of autonomic and sensorimotor processing in the lateral cerebellum. Cell Reports *32*, 107867. https://doi.org/10.1016/j.celrep.2020.107867.

Schonewille, M., Belmeguenai, A., Koekkoek, S.K., Houtman, S.H., Boele, H.J., van Beugen, B.J., Gao, Z., Badura, A., Ohtsuki, G., Amerika, W.E., et al. (2010). Purkinje cell-specific knockout of the protein phosphatase PP2B impairs potentiation and cerebellar motor learning. Neuron *67*, 618–628.

Schonewille, M., Gao, Z., Boele, H.J., Veloz, M.F., Amerika, W.E., Simek, A.A.M., De Jeu, M.T., Steinberg, J.P., Takamiya, K., Hoebeek, F.E., et al. (2011). Reevaluating the role of LTD in cerebellar motor learning. Neuron *70*, 43–50.

Smith, E.E., and Jonides, J. (1999). Storage and executive processes in the frontal lobes. Science *283*, 1657–1661.

Steinmetz, J.E., Logan, C.G., Rosen, D.J., Thompson, J.K., Lavond, D.G., and Thompson, R.F. (1987). Initial localization of the acoustic conditioned stimulus projection system to the cerebellum essential for classical eyelid conditioning. Proc. Natl. Acad. Sci. USA *84*, 3531–3535.

Tavano, A., Grasso, R., Gagliardi, C., Triulzi, F., Bresolin, N., Fabbro, F., and Borgatti, R. (2007). Disorders of cognitive and affective development in cerebellar malformations. Brain *130*, 2646–2660.

ten Brinke, M.M., Boele, H.J., Spanke, J.K., Potters, J.W., Kornysheva, K., Wulff, P., IJpelaar, A.C.H.G., Koekkoek, S.K.E., and De Zeeuw, C.I. (2015). Evolving models of Pavlovian conditioning: cerebellar cortical dynamics in awake behaving mice. Cell Rep. *13*, 1977–1988.

Tsutsumi, S., Hidaka, N., Isomura, Y., Matsuzaki, M., Sakimura, K., Kano, M., and Kitamura, K. (2019). Modular organization of cerebellar climbing fiber inputs during goal-directed behavior. eLife *8*, e47021.

Tzvi, E., Koeth, F., Karabanov, A.N., Siebner, H.R., and Krämer, U.M. (2020). Cerebellar - Premotor cortex interactions underlying visuomotor adaptation. Neuroimage *220*, 117142.

van Alphen, A.M., and De Zeeuw, C.I. (2002). Cerebellar LTD facilitates but is not essential for long-term adaptation of the vestibulo-ocular reflex. Eur. J. Neurosci. *16*, 486–490.

Van Der Giessen, R.S., Koekkoek, S.K., van Dorp, S., De Gruijl, J.R., Cupido, A., Khosrovani, S., Dortland, B., Wellershaus, K., Degen, J., Deuchars, J., et al. (2008). Role of olivary electrical coupling in cerebellar motor learning. Neuron *58*, 599–612.

Wang, X., Novello, M., Gao, Z., Ruigrok, T.J.H., and De Zeeuw, C.I. (2021). Input and output organization of the mesodiencephalic junction for cerebro-cerebellar communication. J. Neurosci. Research. https://doi.org/10.1002/jnr.24993.

Weijnen, J.A.W.M., Wouters, J., and van Hest, J.M.H.H. (1984). Interaction between licking and swallowing in the drinking rat. Brain Behav. Evol. *25*, 117–127.

Witter, L., Canto, C.B., Hoogland, T.M., de Gruijl, J.R., and De Zeeuw, C.I. (2013). Strength and timing of motor responses mediated by rebound firing in the cerebellar nuclei after Purkinje cell activation. Front. Neural Circuits *7*, 133.

Wolpert, D.M., Miall, R.C., and Kawato, M. (1998). Internal models in the cerebellum. Trends Cogn. Sci. *2*, 338–347.

Xia, J., Chung, H.J., Wihler, C., Huganir, R.L., and Linden, D.J. (2000). Cerebellar long-term depression requires PKC-regulated interactions between GluR2/3 and PDZ domain-containing proteins. Neuron *28*, 499–510.

Xu, N.L., Harnett, M.T., Williams, S.R., Huber, D., O'Connor, D.H., Svoboda, K., and Magee, J.C. (2012). Nonlinear dendritic integration of sensory and motor input during an active sensing task. Nature *492*, 247–251.

Yang, Y., and Lisberger, S.G. (2014). Purkinje-cell plasticity and cerebellar motor learning are graded by complex-spike duration. Nature *510*, 529–532.

Yu, F., Jiang, Q.J., Sun, X.Y., and Zhang, R.W. (2015). A new case of complete primary cerebellar agenesis: clinical and imaging findings in a living patient. Brain *138*, e353.

Zeng, H., Chattarji, S., Barbarosie, M., Rondi-Reig, L., Philpot, B.D., Miyakawa, T., Bear, M.F., and Tonegawa, S. (2001). Forebrain-specific calcineurin knockout selectively impairs bidirectional synaptic plasticity and working/episodic-like memory. Cell *107*, 617–629.

Zhou, H., Lin, Z., Voges, K., Ju, C., Gao, Z., Bosman, L.W.J., Ruigrok, T.J.H., Hoebeek, F.E., De Zeeuw, C.I., and Schonewille, M. (2014). Cerebellar modules operate at different frequencies. eLife *3*, e02536.

Zhou, P., Resendez, S.L., Rodriguez-Romaguera, J., Jimenez, J.C., Neufeld, S.Q., Giovannucci, A., Friedrich, J., Pnevmatikakis, E.A., Stuber, G.D., Hen, R., et al. (2018). Efficient and accurate extraction of in vivo calcium signals from microendoscopic video data. eLife *7*, e28728.

STAR★METHODS

KEY RESOURCES TABLE

REAGENT or RESOURCE	SOURCE	IDENTIFIER
Chemicals, peptides, and recombinant proteins		
Bupivacaine	Actavis	RVG 20949
Buprenorphine	Indivior	RVG 08725
Isoflurane	Pharmachemie	45.112.110
Kwik-Cast Silicone Sealant	World Precision Instruments	KWIK-CAST
Kwik-Sil Silicone Adhesive	World Precision Instruments	KWIK-SIL
Lidocaine	Braun	RVG 07831
D-Mannitol	Merck (Sigma-Aldrich)	CAS 69-65-8
Optibond adhesive	Kerr Corporation	33381E
Rimadyl	Pfizer	CAS 53716-49-7
Superbond C&B	Sun Medical	7100
Experimental models: Organisms/strains		
C57BL6/J mice	Charles Rivers	IMSR_JAX:000664
Tg(Pcp2-cre)2Mpin; Gt(ROSA)26Sor$^{tm27.1(CAG-OP4*H134R/tdTomato)Hze}$	Witter et al., 2013, Own breeding	n/a
Tg(Pcp2-cre)2MPin;Ppp3r1^{tm1Stl}	Schonewille et al., 2010, Own breeding	n/a
Tg(Pcp2-cre)2MPin;Gria2Δ7 knock in	Xia et al., 2000, Own breeding	n/a
Recombinant DNA		
AAV1.CMV.PI.Cre.rBG	Addgene	Addgene_105530
AAV.Syn.GCaMP6f.WPRE.SV40	Addgene	Addgene_100837
Software and algorithms		
BIOTACT Whisker Tracking Tool (BWTT)	Perkon et al., 2011	http://bwtt.sourceforge.net/
Accelerated BWTT	(Romano et al., 2020)	https://gitlab.com/neurocomputing-lab/whisker/bwtt-acceleration and https://github.com/elifesciences-publications/BWTT_PP
Constrained Nonnegative Matrix Factorization for microEndoscopic data (CNMF-E)	Zhou et al., 2018; (Pnevmatikakis and Giovannucci, 2017)	https://github.com/zhoupc/CNMF_E
Non-Rigid Motor Correction (NorMCorre)	(Pnevmatikakis and Giovannucci, 2017)	https://github.com/flatironinstitute/NoRMCorre
MacroStitching	This paper	https://figshare.com/articles/online_resource/MacroStitching_ijm/16998697
Excel	Microsoft	n/a
Illustrator	Adobe	n/a
ImageJ	NIH	https://imagej.nih.gov/ij/
MATLAB	MathWorks	n/a
SigmaPlot	Systat Software	n/a
SpikeTrain	Neurasmus	n/a
SPSS Statistics	IBM	n/a

RESOURCE AVAILABILITY

Lead contact

Further information and requests for resources and reagents should be directed to and will be fulfilled by the lead contact, Laurens Bosman (l.bosman@erasmusmc.nl).

Materials availability

This study did not generate new unique reagents.

Data and code availability

- Data are available upon request from the lead contact.
- All original code has been deposited at Figshare and is publicly available as of the date of publication. DOIs are listed in the Key Resources Table.
- Any additional information required to reanalyze the data reported in this paper is available from the Lead Contact upon request.

EXPERIMENTAL MODEL AND SUBJECT DETAILS

All experiments were performed on adult mice with a C57BL6/J background. *Pcp2-Pppr3r1* (Tg(Pcp2-cre)2MPin;Ppp3r1^{tm1Stl}, formerly also known as *L7-PP2B*) KO mice lacked functional PP2B specifically in their PCs. They were created by crossing mice in which the gene for the regulatory subunit (CNB1) of PP2B was flanked by *LoxP* sites (Zeng et al., 2001) with transgenic mice expressing Cre-recombinase under control of the *Pcp2* (*L7*) promoter (Barski et al., 2000), as described in Schonewille et al. (2010). Learning curves of L7-PP2B mice (4 males and 5 females) were compared with their control littermates (5 males and 4 females) that were trained together. The training curves of the wild-type mice (Figure 2) were constructed of the wild-type littermates of the *Pcp2-Ppp3r1* mice, combined with five extra male control mice. For the naive and untrained groups, we used 4 (2 males and 2 females), and 6 (3 males and 3 females) control mice, respectively. Four male wild-type mice were used for the calcium imaging experiments.

Gria2-Δ7 knock-in (*GluR2*Δ7) mice lack the last seven amino acids at the intracellular C-terminal tail, thereby disrupting the interaction of GluA2 with PICK1 and GRIP1/2, in turn disrupting the internalization of AMPA receptors, which impairs parallel fiber-to-PC LTD (Boele et al., 2018; Xia et al., 2000; Schonewille et al., 2011). *Gria2*-Δ7 KI mice (8 males and 8 females) were also trained together with their littermates (3 males and 10 females) in order to compare their learning curves. The wild-type mice of this group was used for the electrophysiological recordings with omitted and unexpected rewards.

Optogenetic experiments were performed on transgenic mice (11 males and 2 females) that expressed Channelrhodopsin2 (ChR2) under the *Pcp2* promoter (Witter et al., 2013).

The animals were group housed until magnetic pedestal placement; after that they were single housed in a vivarium with controlled temperature and humidity and a 12/12h light/dark cycle. All recordings and behavioral experiments were performed in awake, head restrained mice with an age between 11 and 35 weeks. All mice were healthy and specific pathogen free (SPF). All experimental procedures were approved *a priori* by an independent animal ethical committee (DEC-Consult, Soest, the Netherlands) as required by Dutch law and conform the relevant institutional regulations of the Erasmus MC and Dutch legislation on animal experimentation. Permission was filed under the license numbers EMC3001, AVD101002015273 and AVD1010020197846.

METHOD DETAILS

Habituation and water restriction

Mice received a magnetic pedestal for head fixation, attached to the skull above bregma using Optibond adhesive (Kerr Corporation) under isoflurane anesthesia (2%–4% v/v in O_2). Postsurgical pain was treated with carprofen (Rimadyl, Pfizer) and lidocaine (Braun) and two days of recovery followed the procedure. In order to reduce the stress level during training, the experimenter began to handle mice a week before the start of the actual training for approximately 15 minutes per mouse per day. Starting from three days before the training, the water bottles were removed from the lid of the cages and the body weight of mice was daily monitored and mice were head fixed and restrained for 15 minutes each day; during this time, water was available from the lick-port positioned in front of the mouse. Mice that did not drink during this time received a controlled amount of water in their cages; in total mice received a daily amount of 1 mL of water per 20 g body weight.

Behavioral paradigm and surgical procedures

Mice were trained for 18-20 days to associate the position of a pole with the presence or absence of a water reward. During training, go and no-go trials were randomly intermingled. In go trials, a pole was raised in the middle of the whisker field and the mice could trigger a water reward by licking during the response interval. An important difference with paradigms generally described in related studies (Heffley and Hull, 2019; Heffley et al., 2018; Kostadinov et al., 2019; Larry et al., 2019) during which water was given irrespective of the action of the mice, is that, in our paradigm, the water delivery was triggered by making a tongue protrusion, so that our mice could not use the presence of water nor the valve click as a cue. During no-go trials, mice were not supposed to lick and licking was consequently not rewarded. Each trial, whether go or no-go, started with a clearly audible sound made by the pneumatic device raising the pole. The pole was constructed so that the location and the characteristics of the sound were identical between go and no-go trials. Licking during the 300 ms period following trial start, announced by the sound cue, was not allowed and induced early termination of the trial and an aversive air puff to the nose of the mouse. During the first two days of training the aversive puff was

omitted to facilitate the participation to the task. During training, body weight and health condition of mice were monitored and mice not cooperating or not in good health condition were taken out of the experiment (6 out of 72).

At the end of the training mice received the water bottle in their cages for two days. Once recovered from the water restriction regime, a craniotomy was performed to expose cerebellar crus 1 and crus 2 on the right side. As this procedure was longer and more invasive than pedestal placement, the analgesia previously mentioned was complemented with bupivacaine (Actavis, Parsippany-Troy Hills, NJ, USA) and buprenorphine ("Temgesic," Indivior, Richmond, VA, USA), and the recovery period was three days. The craniotomy was cleaned and afterward covered with Kwik-Cast (World Precision Instrument, Sarasota, FL, USA).

After mice recovered, the water restriction regime restarted. A retraining phase of two to five days preceding the electrophysiology allowed us to verify, apart from the health condition of our mice, that the participation level was suitable for efficient electrophysiological recordings. During electrophysiological recordings, trained mice were tested using the same type of trials as during training. In a subset of mice, however, we inverted the outcome of the mouse response in go and no-go trials, resulting in omitted and unexpected rewards, respectively. Normal and inverted trials occurred in a random sequence, with inverted trials accounting for 20% of the total number of trials.

In naive and in untrained mice, pedestal placement and craniotomy were performed in a single session, using the anesthetic and analgesic regime of the craniotomy as described above. After three days of recovery, naive mice were habituated daily to head fixation in the recording setup during three days. On the fourth day, electrophysiological recordings were made while the mice received for the sensory stimuli as previously described.

The untrained mice were treated largely similar as the naive mice, but during their habituation sessions, they were accustomed to the presence and working of the lick port in the recording setup. Like the naive mice, they were not exposed to the sensory stimuli before the electrophysiological recording session. Unlike in all other experiments in this study, the untrained mice received only go trials, and they did not have to lick first to trigger water reward. Instead, the water rewards were triggered at random times during the response window. An equal amount of water rewards was given at random times during inter-trial intervals, so completely uncoupled from the sensory stimuli.

Optogenetic stimulation

After craniotomy and retraining, *Pcp2-Cre/Ai27* (Tg(Pcp2-cre)2Mpin; Gt(ROSA)26Sor$^{tm27.1(CAG-OP4*H134R/tdTomato)Hze}$) mice underwent to two task sessions (consecutive days) during light stimulation. An optic fiber (diameter 400 μm, Thorlabs, Newton, NJ, USA) was placed in the middle of the craniotomy perpendicular to the cerebellar surface. Three conditions were randomly intermingled for both go or no-go trials: a control condition of unaltered go or no-go trials and two conditions where a pulse of blue LED light (λ = 470 nm, duration = 250 ms, p = 5 mW) was given. During the first session, the light pulse was delivered either at time 0 ms (together with the acoustic cue) or after 300 ms (when the pole reached the top position); during the second session the light turned on either at 0 ms or at 550 ms during the response window, when licking was generally already ongoing. After the session the craniotomy was rinsed with saline and closed with Kwik-Cast. PCs of these mice were recorded in a subsequent session one to three days later.

Electrophysiology

Electrophysiological recordings were performed in awake mice using quartz-coated platinum/tungsten electrodes (R = 2-5 MΩ, outer diameter = 80 μm, Thomas Recording, Giessen, Germany). Electrodes were placed in an 8x4 matrix (Thomas Recording), with an inter-electrode distance of 305 μm. Prior to the recordings, the mice were lightly anesthetized with isoflurane to remove the dura mater, bring them in the setup and place the electrodes on the surface of the cerebellum. Recordings started at least 60 min after termination of anesthesia and were made in crus 1 and crus 2 ipsilateral to the side of the whisker stimulation at a minimal depth of 500 μm. The voltage signal was digitized at 25 kHz, using a 1-6,000 Hz band-pass filter, 22x pre-amplified and stored using a RZ2 multi-channel workstation (Tucker-Davis Technologies, Alachua, FL). Once awake, mice attention was triggered by randomly delivering few drops of water until they spontaneously started seeking for water. Once good stable signal was found from at least one cells and anyway not after more than 90 minutes from the moment we remove the anesthesia, the behavioral session was started and continued until mice stopped drinking and we collected a certain amount of trials in the absence of licking responses.

Behavioral data analysis

Licking bouts were defined as sequences of licks with intervals < 500 ms. Trials in which the trial start fell within an ongoing licking bout (that started at least 20 ms before the sound cue was given) were ignored for the calculation of performance.

After optogenetic stimulation we were interested in observing if any changes were induced by the light in the licks' distribution following the cues or within ongoing bouts. We therefore built peri-stimulus time histograms (PSTHs, 50 ms bins) of the latencies of licks from trial onset with and without light stimulation, then compared the licking probability in the two 250 ms windows starting from 0 ms or 550 ms.

Behavioral performance was calculated as 1 - (number of trials with early lick + number of false alarm trials) / number of hit trials.

Electrophysiological data analysis

Spikes were detected offline using SpikeTrain (Neurasmus, Rotterdam, the Netherlands). A recording was considered to originate from a single PC when it contained both CSs (identified by stereotypic waveform, overshooting and the presence of spikelets) and SSs, and in which each CS was followed by a pause of at least 8 ms before SS firing resumed. When comparing two or more conditions, only recordings containing at least 8 events per condition were included in each group. We generally used bins of 10 ms to visualize SSs and of 15 ms for CSs and licks. In order to compare the modulation from different cells or evoked by different triggers, PSTHs have been normalized on the mean firing frequency calculated in a 2 s interval preceding the second before the trigger. To compare CSs modulation to trials cues, peaks have been detected in the two temporal windows of interest (20-100 ms and 240-320 ms after trial start) as maximum bin value. A cell was considered modulating when in one or both the temporal windows the maximal CS modulation exceeded the mean baseline frequency by at least 3 sd. SSs virtually always showed some degree of modulation, so that we did not separate them into responsive and non-responsive cells, unless noted otherwise.

Miniscope imaging

Calcium transients were imaged daily in a group of four mice using the NINscope miniscope using procedures described previously (de Groot et al., 2020). Briefly, mice were anesthetized with isoflurane in a stereotactic apparatus and a pedestal for head fixation was mounted. A 2 mm round craniotomy was made centered above cerebellar lobule crus 1 to inject virus (AAV1.CAG.FLEX. GCaMP6f/AAV1.CMV.PI.Cre.rBG mixed 1:1, which was diluted 1:3 in saline) for transduction of PCs with GCaMP6f, and to mount a gradient index (GRIN) lens. Fifteen minutes prior to virus injection, D-mannitol (15% in saline) was injected i.p. to facilitate virus diffusion (Kuhn et al., 2012). Virus was injected at four locations. At each location 25 nL of virus was injected once at 350, twice at 300 and once at 250 μm depth at a rate of 25 nL/min with a Nanoject II Auto-Nanoliter Injector (Drummond Scientific Company, USA). After injection of the virus, a 1.8 mm GRIN lens was implanted. Kwik-Sil (WPI, USA) was applied around the edges of the craniotomy and the lens. Subsequently, the lens was secured by applying dental cement (Super-Bond C&B, Sun Medical, Japan). The lens was covered with Kwik-Cast (WPI, USA) for protection. Two to three weeks after viral injection a baseplate was mounted in an optimal location and secured with dental cement.

Before training commenced, mice were first habituated for a week to being head-fixed using the head pedestal and for the mice to discover the location of the lick-port and water reward. Mice were then subjected to the same training protocol as described before, but now with a mounted miniscope for calcium imaging. For every session, 220 frames were collected at 30 Hz. Recordings began 3 s before presentation of the first stimulus. Imaging continued for a period of twenty days from commencement of training.

Extraction and analysis of calcium transients

Raw data were motion-corrected using noRMCorre (Pnevmatikakis and Giovannucci, 2017) and calcium transients were extracted using CNMF-E (Zhou et al., 2018). In order to compare the modulation of the same cells across three different training sessions motion corrected frames recorded at days 4, 13 and 20 of training were concatenated in order to obtain one large video; between-sessions misalignment was corrected using custom code (MacroStitching) in ImageJ: the frames composing each session were averaged, then the three averages were manually overlapped based on landmarks and the exceeding pixels on the x and y axis were cropped from each frame. Having obtained a single video, we ran CNMF-E on these aligned data to extract spatial footprints of PC dendrites and their corresponding signals across the three sessions. Variations in the baseline signal present across different sessions were subtracted (mean of sliding median and sliding minimum, 25 frames sliding window). Deconvolved transients were used to determine the onset of the calcium transients. Bin size for peri-stimulus histograms was set at 33 ms given a 30 Hz acquisition.

Whisker movement tracking

Whisker movements were tracked as described previously (Romano et al., 2020) using the BIOTACT Whisker Tracking Tool (Perkon et al., 2011) in combination with an acceleration version of the BIOTACT code. For the purposes of this work, the whisker movements were captured as the average angle of all trackable whiskers per frame. Whisker videos were recorded with a frame rate of 750 frames per second.

QUANTIFICATION AND STATISTICAL ANALYSIS

Data distributions were tested for normality using Kolmogorov-Smirnov tests, and in case of non-normal distributions, non-parametric tests were used. Tests were two sided. We considered a p value < 0.05 as statistically significant for tests without multiple comparisons. Unless stated otherwise, we have used the Benjamini-Hochberg method to correct for multiple comparisons, and adapted the threshold for significance accordingly, as indicated throughout the text. The specific test used at each instance, is mentioned in the text and in Tables S1 and S2.

Cell Reports, Volume *37*

Supplemental information

Purkinje cells translate subjective salience into readiness to act and choice performance

Lorenzo Bina, Vincenzo Romano, Tycho M. Hoogland, Laurens W.J. Bosman, and Chris I. De Zeeuw

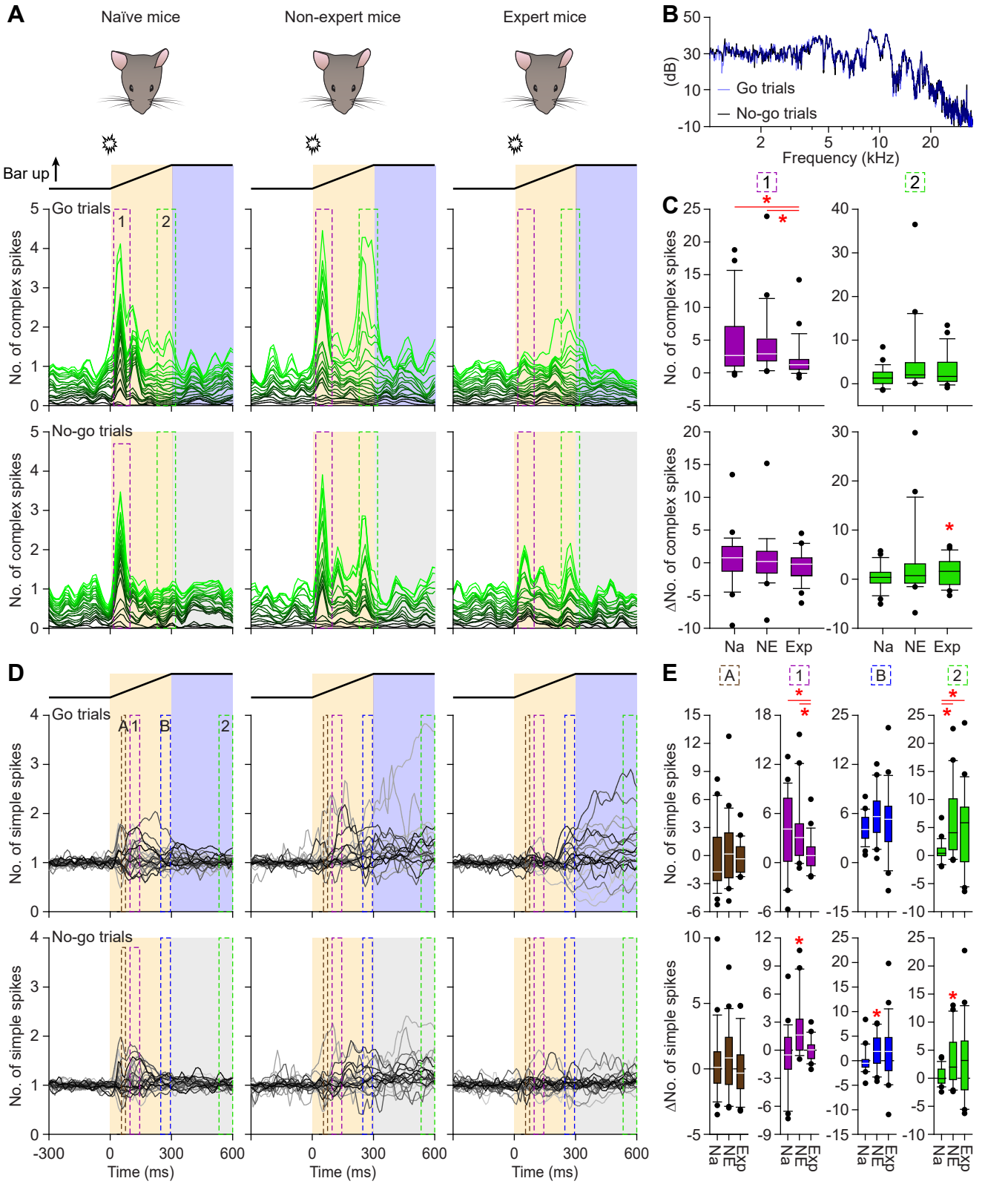

Figure S1. Changes in CS and SS timing during learning. Related to Figures 1 and 3.

A. Stacked line plots of CS firing in naïve (left), non-expert (middle) and expert (right) mice (see Fig. 3E) during go and no-go trials. Each line represents the peristimulus time histogram of a single PC. The PCs are sorted based upon the maximal CS response during go trials and normalized to the pre-trial activity and scaled so that the upper (brightest) line represents the population average. It is clear that the first (auditory) cue at the start of the trial has a stronger impact than the second (tactile) cue. All 24 recorded PCs are included in this analysis, irrespective of whether they displayed a statistically significant response. **B.** The sound of the stimulator was similar during go and no-go trials, as evinced from spectrograms derived from 10 go and 10 no-go trials. For this analysis, we evaluated 140 ms at the trial start. **C.** Top row: box plots of the maximal CS peak during the first (20-100 ms, left) and the second (240-320 ms, right) time window. Bottom row: box plots of the difference in maximal response for the for the first (left) and second (right) time window between go and no-go trials. **D** and **E.** The same for the SS activity. For SSs, we evaluated four time windows, as indicated in **D** and explained in Table S1. * indicates statistical significance, see Table S1. Na = naïve, NE = non-expert, Exp = Expert.

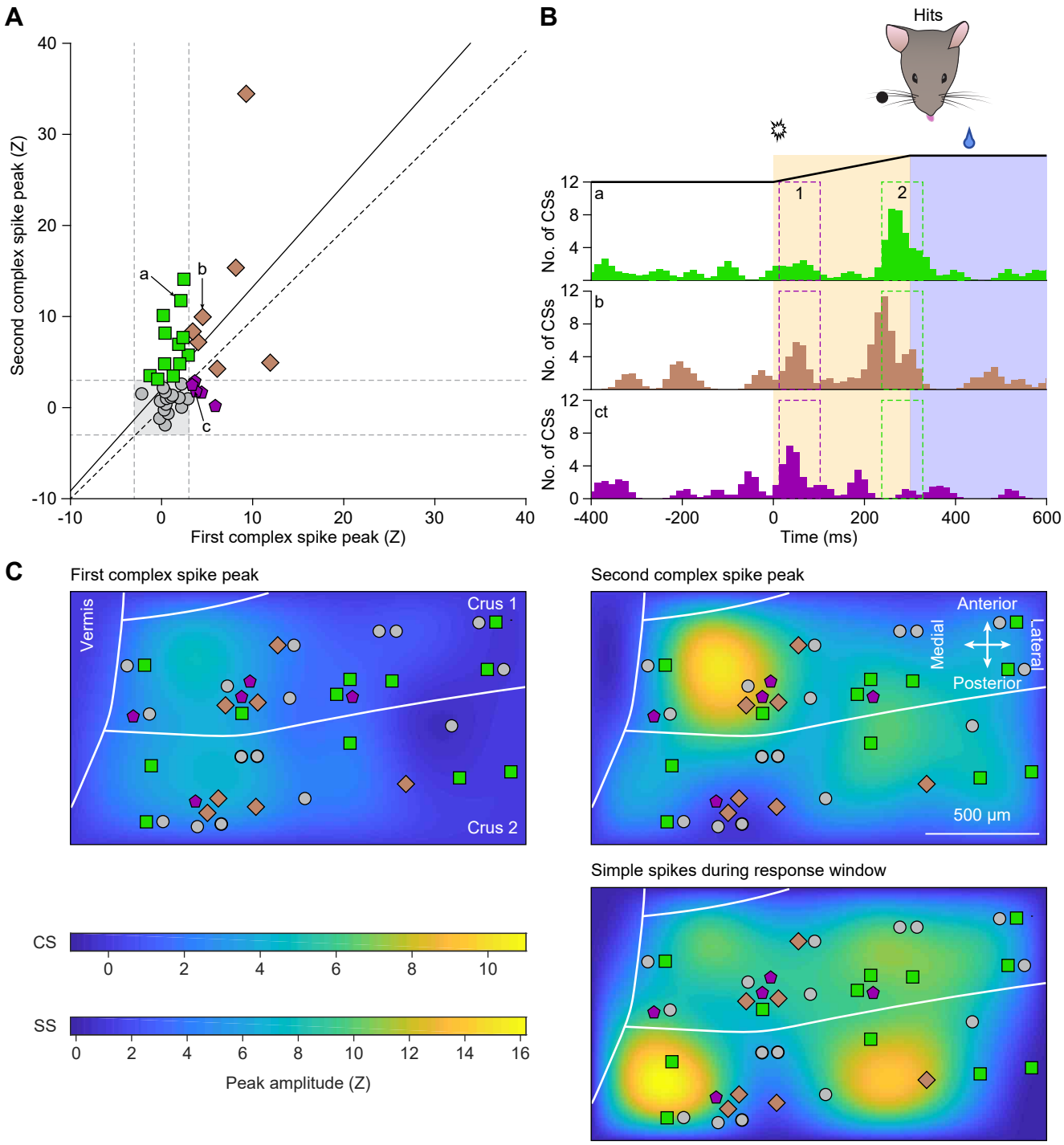

Figure S2. Spatiotemporal aspects of CSs and SSs. Related to Figure 3.

A. At the level of individual PCs, the strength of the first (sound-evoked; 20-100 ms) and second (touch-induced; 240-320 ms) CS peak (see Fig. 3C) were weakly correlated. The "purple cells" preferentially fired during the first time window, the "green cells" during the second, and the "brown cells" during both. The solid line indicates the linear regression line (r = 0.35, p = 0.019, Spearman correlation test), the dotted line is at 45°, indicating equal strength of both peaks. **B.** Peri-stimulus time histograms of three example PCs. The numbers refer to their location in **A**. **C.** Relative strength of the first and second CS peak, respectively, as distributed over the area of crus 1 and crus 2, as well as that of the SS modulation during the response window. The approximate recording locations of the PCs are indicated using the same color/shape code as in **A.** Recording locations that were very close together were displayed minimally to improve visibility.

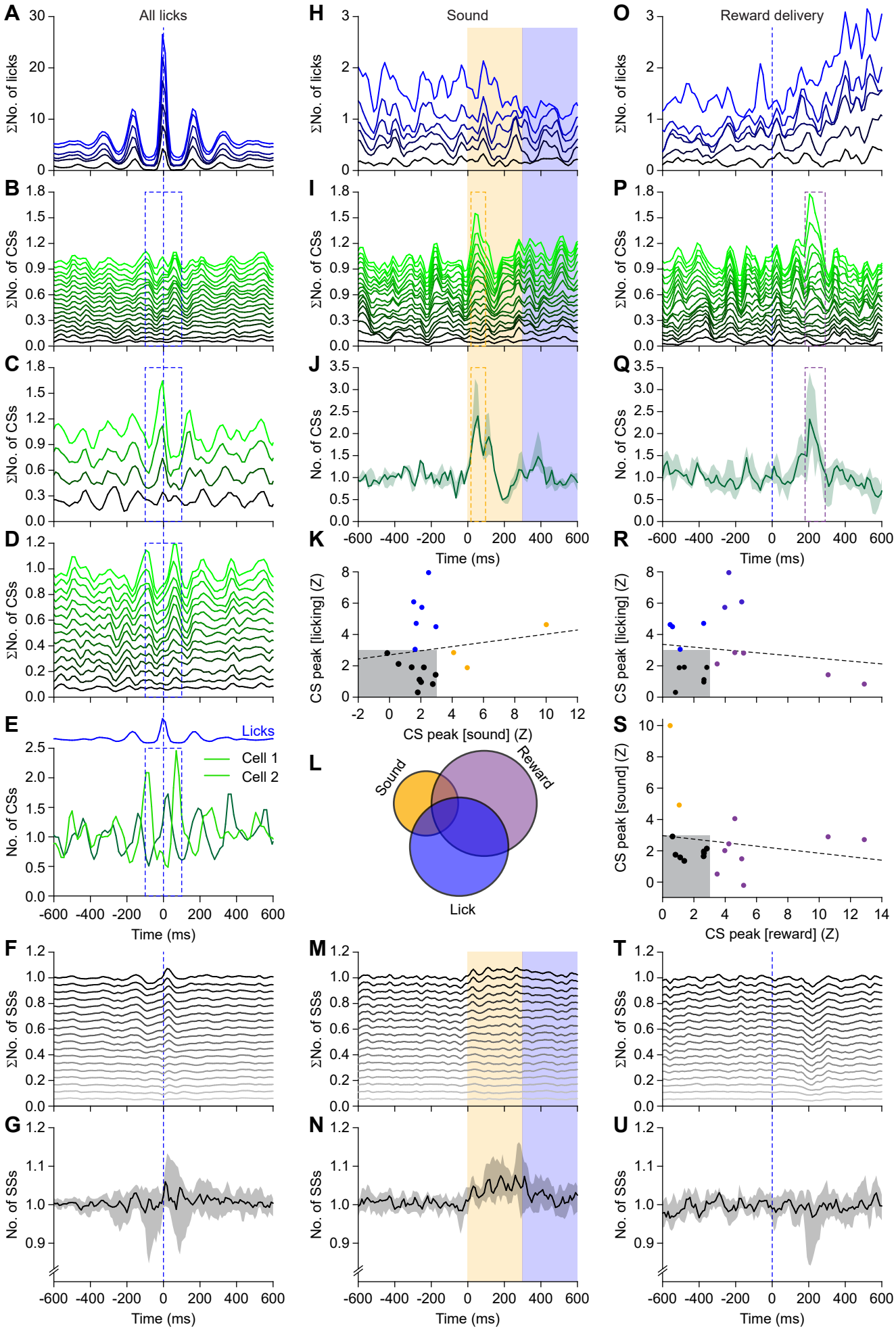

Figure S3. Lick- and reward-related PC activity in untrained mice. Related to Figure 3.

Figure S3. Lick- and reward-related PC activity in untrained mice. Related to Figure 3.

A. Stacked autocorrelograms of all licks. Each line represents one of the 6 untrained mice – mice that were habituated to the setup and accustomed to lick from the lick port, but that had not been exposed to the sensory stimuli of our paradigm before the recording session started. The autocorrelograms emphasize the rhythmic character of licking. **B.** Stacked line plots of the CSs fired by 16 PCs during licking. Some PCs preferentially fired during tongue protrusion (**C**), while others fired more during tongue retraction (**D**). **E.** Both types of PCs were present in individual mice, as illustrated by two simultaneously recorded PCs. **F.** Stacked line plots of the SSs fired during licking, summarized as median firing rate after normalization to baseline firing (**G**). Shading indicates inter-quartile range. **H.** Stacked line plot of licking aligned on the sound cue signaling trial start. Note that the untrained mice were not previously accustomed to the trial structure, and were often licking during the inter-trial intervals. **I.** CS responded to the sound, but hardly to the tactile cue (at the end of the 300 ms no-lick period following the sound cue). Summarized as median activity of the 3 PCs that showed statistically significant responses (**J**). Shading indicates inter-quartile range. **K.** Scatter plot of the amplitude of the sound-induced CS peak (x-axis) vs. that during the time interval around licking (blue rectangle in B). Linear regression: r = 0.13, p = 0.590. **L.** Venn diagram showing the partial overlap in statistically significant CS encoding of acoustic responses, reward detection, and licking, at the level of individual PCs. **M.** Stacked line plots of SS firing aligned on trial start, and summarized as median firing rate after normalization to baseline firing (**N**). Shading indicates inter-quartile range. **O.** Rewards were given at random moments during the response window, as well as during the inter-trial interval, which resulted – with some delay – in increased licking. **P.** CS responded to reward delivery with a delay of around 200 ms. Summarized as median activity of the 8 PCs that showed statistically significant responses during the interval as indicated by the purple rectangle (**Q**). Shading indicates inter-quartile range. **R.** Scatter plot of the amplitude of the reward-induced CS peak (x-axis) vs. that during the time interval around licking (blue rectangle in **B**). Linear regression: r = 0.14, p = 0.578. **S.** Scatter plot of the amplitude of the reward-induced CS peak (x-axis) vs. that triggered by the sound (y-axis). Linear regression: r = 0.17, p = 0.499. **T.** Stacked line plots of SS firing aligned on trial start, and summarized as median firing rate after normalization to baseline firing (**U**). Shading indicates inter-quartile range.

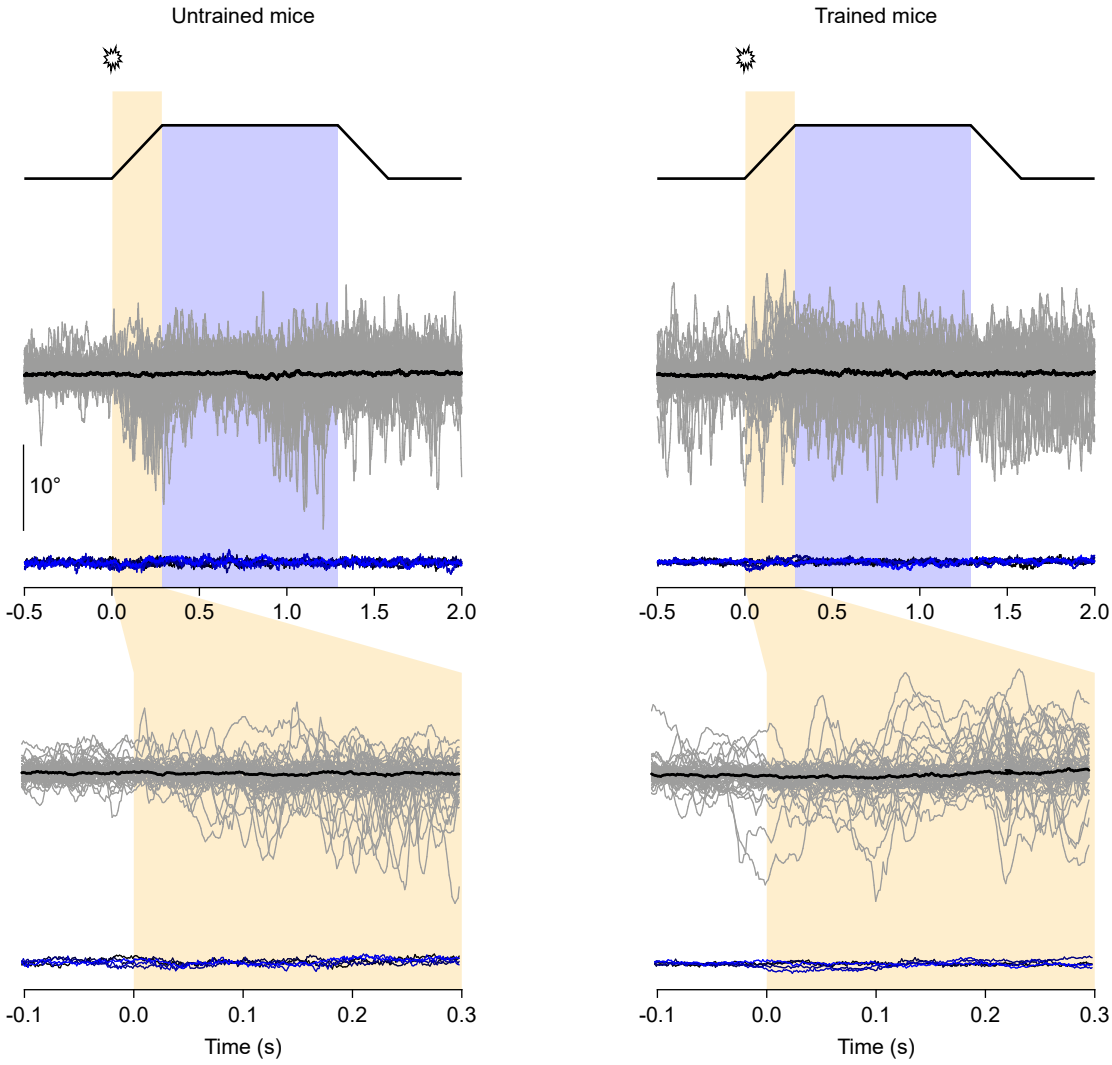

Figure S4. Whisker movements in untrained and trained mice. Related to Figure 3.
In a subset of 5 untrained and 5 trained mice, whisker movements were recorded using a high-speed video-recording. Whisker movements were tracked offline and the average angle of all trackable whiskers on the side of the stimulator are shown. The grey traces show the first 50 trials during the electrophysiological recording session of an exemplary mouse of each group. The mean of these mice are plotted with black lines, demonstrating no stereotypic movement at trial start. The average movements of all five mice are shown in blue-black shades underneath. In none of the mice, indications for a putative acoustic startle response could be observed.

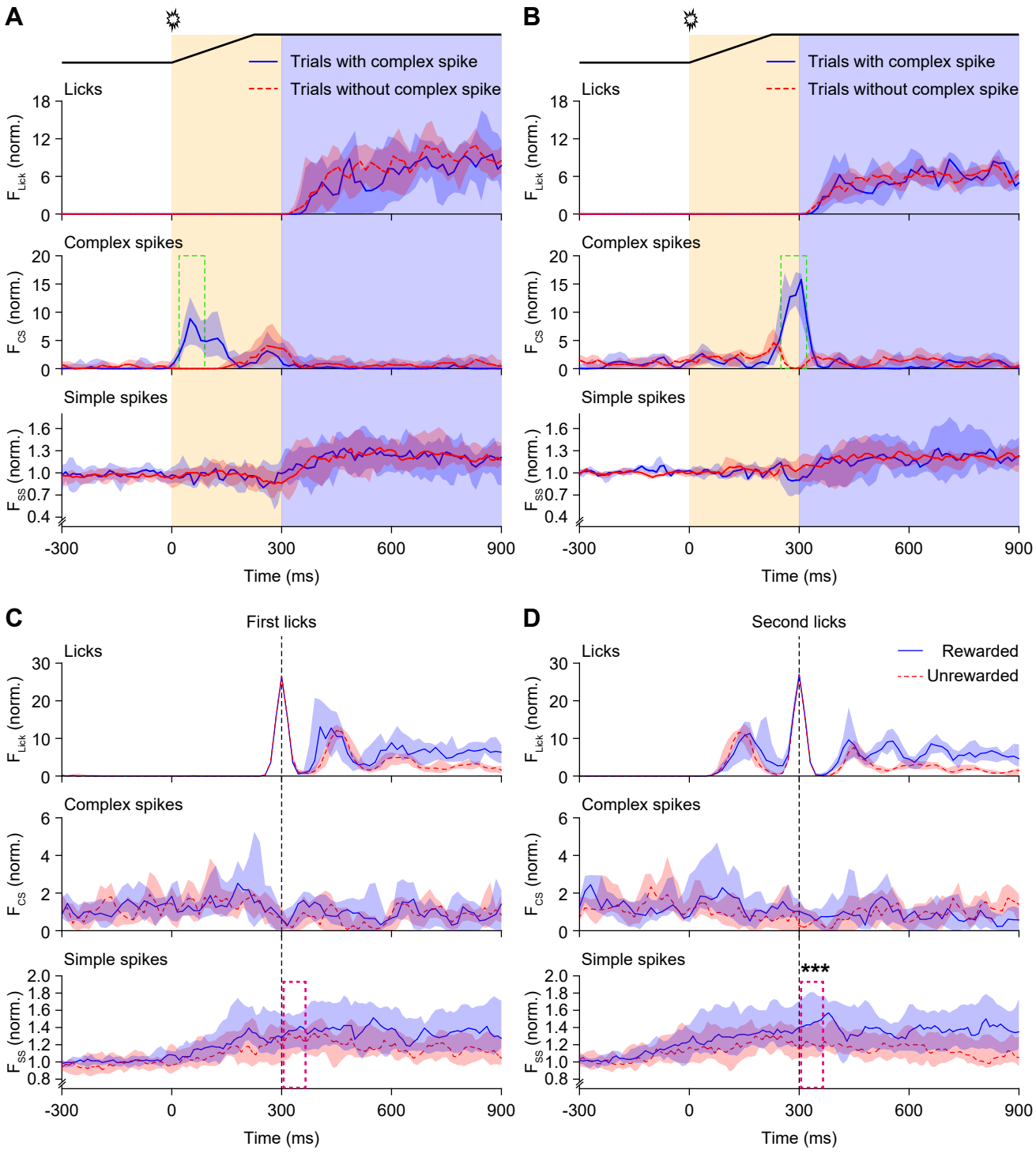

Figure S5. Differential CS and SS firing. Related to Figure 4.
Comparing the trials during which a CS was fired after sound (**A**) or touch (**B**) with those trials that lacked a CS in that interval did not reveal any obvious difference in licking behavior. Peri-stimulus histograms of licks, CSs and SSs triggered on the first (**C**) or second (**D**) lick of bouts that were rewarded (blue) or unrewarded (red). During rewarded bouts, the first lick triggered a water reward. Rewarded lick bouts lasted longer than unrewarded ones. Note that the SSs after the second lick – thus at the moment that the mouse noticed that it got a reward or not – differed between rewarded and unrewarded licks (5-65 ms after detection of second lick: p = 0.007, W = 129, n = 19 PCs, Wilcoxon matched-pairs test).

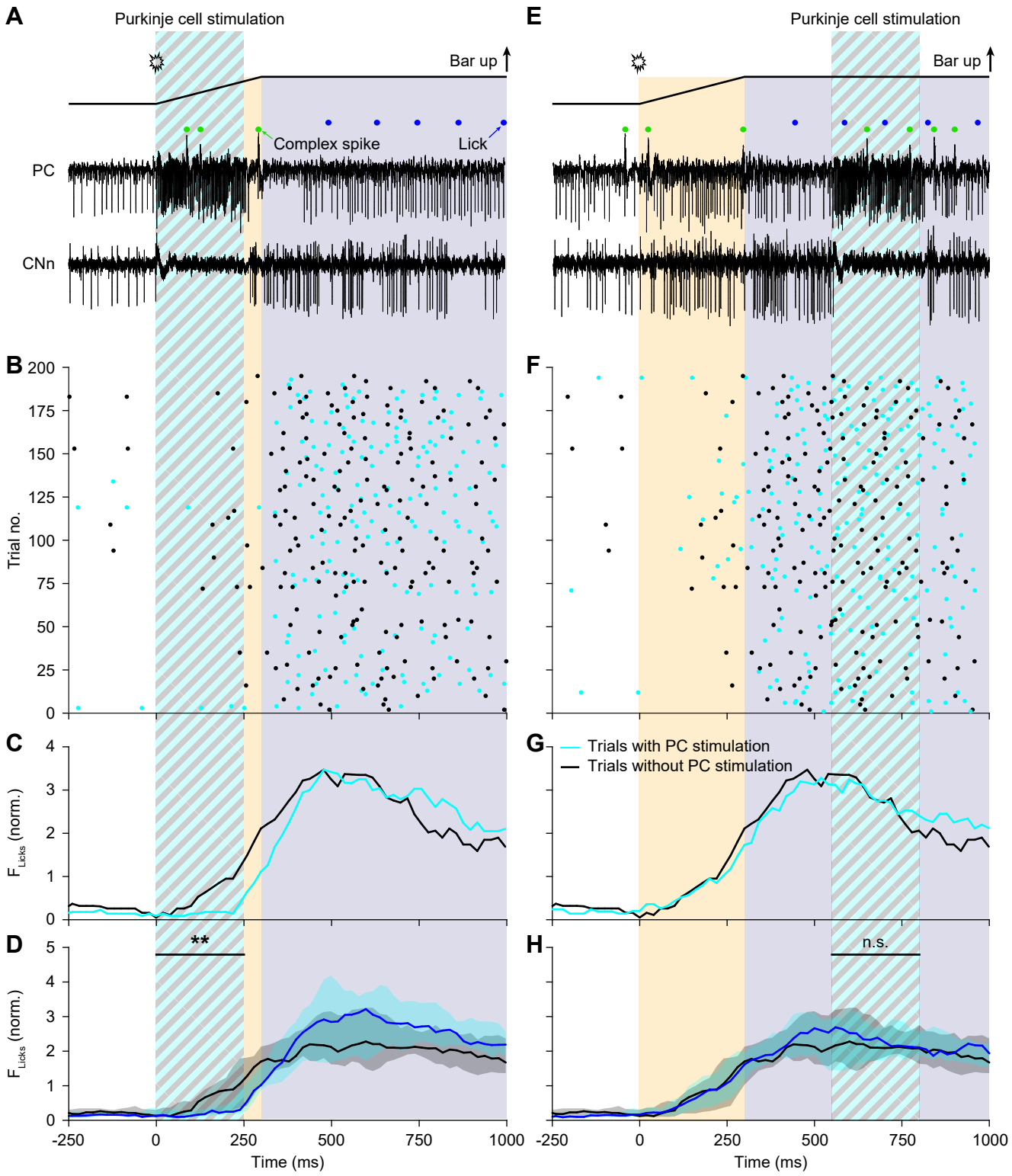

Figure S6. Optogenetic stimulation of PCs delays the onset of licking, but does not interrupt ongoing bouts. Related to Figure 4. Optogenetic stimulation of crus 1 and crus 2 in the lateral hemispheres of Pcp2-ChR2 mice that expressed Channelrhodopsin specifically in their PCs induced a transient increase in PC SS firing and subsequently a decrease in activity of the downstream cerebellar nucleus neurons (CNn). We segregated between stimuli given at the start of licking bouts (**A**-**D**) and during ongoing licking bouts (**E**-**H**). Increased SS firing induced a delay in the onset of licking, but did not affect ongoing lick bouts. Traces (**A** and **E**) and raster plots (**B** and **F**) are all from the same experiment. In the raster plots, black dots indicate licks during trials without optogenetic stimulation, and cyan dots licks during trials with stimulation. Traces with and without optogenetic stimulation were randomly intermingled. **C** and **E.** Peri-stimulus histograms of the exemplary mouse, and **D** and **H** represent convolved medians of 9 mice with the shaded areas indicating the interquartile ranges.

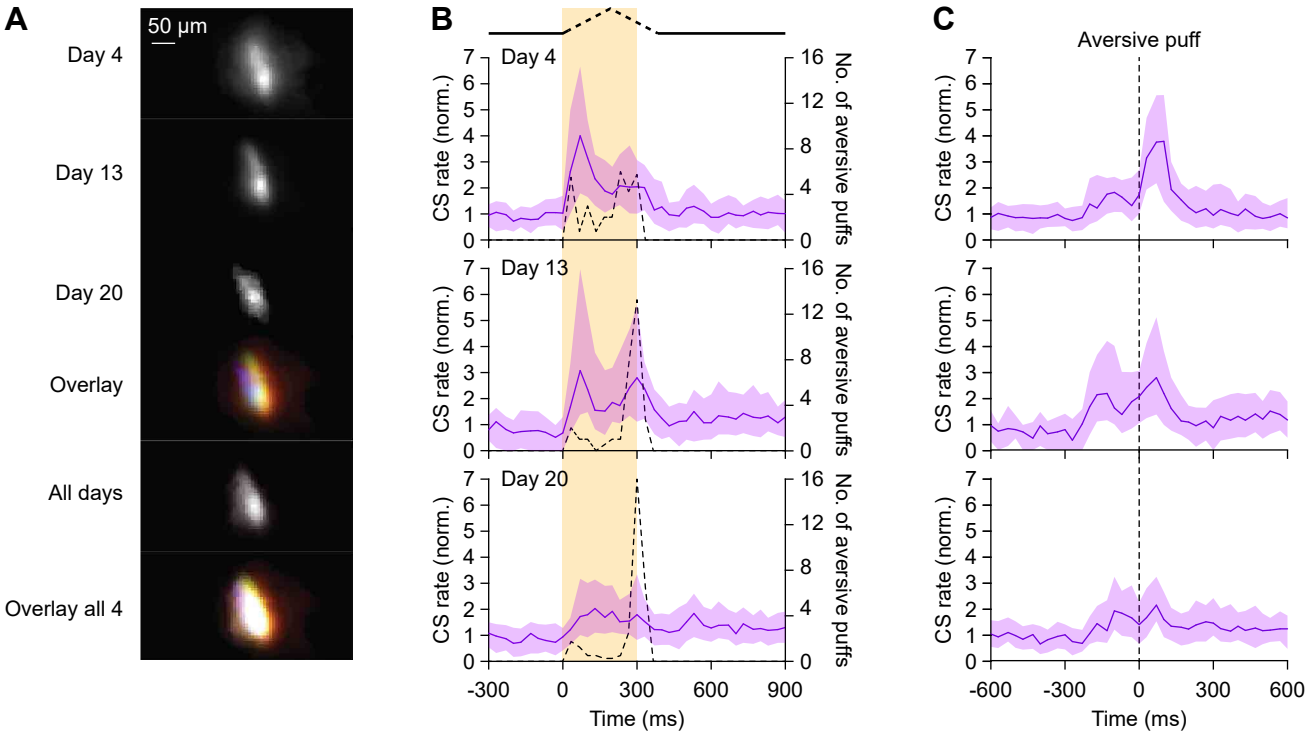

Figure S7. Impact of aversive puff diminishes with training. Related to Figure 6.

A. The same PC dendrite retrieved from recordings at the 4th, 13th and 20th day of recording, and its overlay (copied from Figure 6C). Underneath is the same dendrite extracted from the concatenated video of these three days of recording (see STAR Methods), and the overlay of all conditions. Together, this illustrates the consistency of the location and shape of the same PC over the training. **B.** When a mouse licked during the no-lick period of 300 ms following trial start, it received an aversive air puff to its nose, and the trial was aborted without the option to get a water reward. The dotted lines indicate the histogram of the occurrences of aversive puffs. Note that the aversive puffs were only applied during the no-lick period, but are indicated here with the same temporal resolution as the calcium imaging (30 Hz). Although early licking remained, the impact of the aversive puffs on CS firing (as measured with a miniscope, see Figure 6) strongly diminished with time. **C.** This diminishing effect of the aversive puff on CS firing was further substantiated by triggering CS firing on the aversive puff. For both panels, only trials with aversive puffs were analyzed.

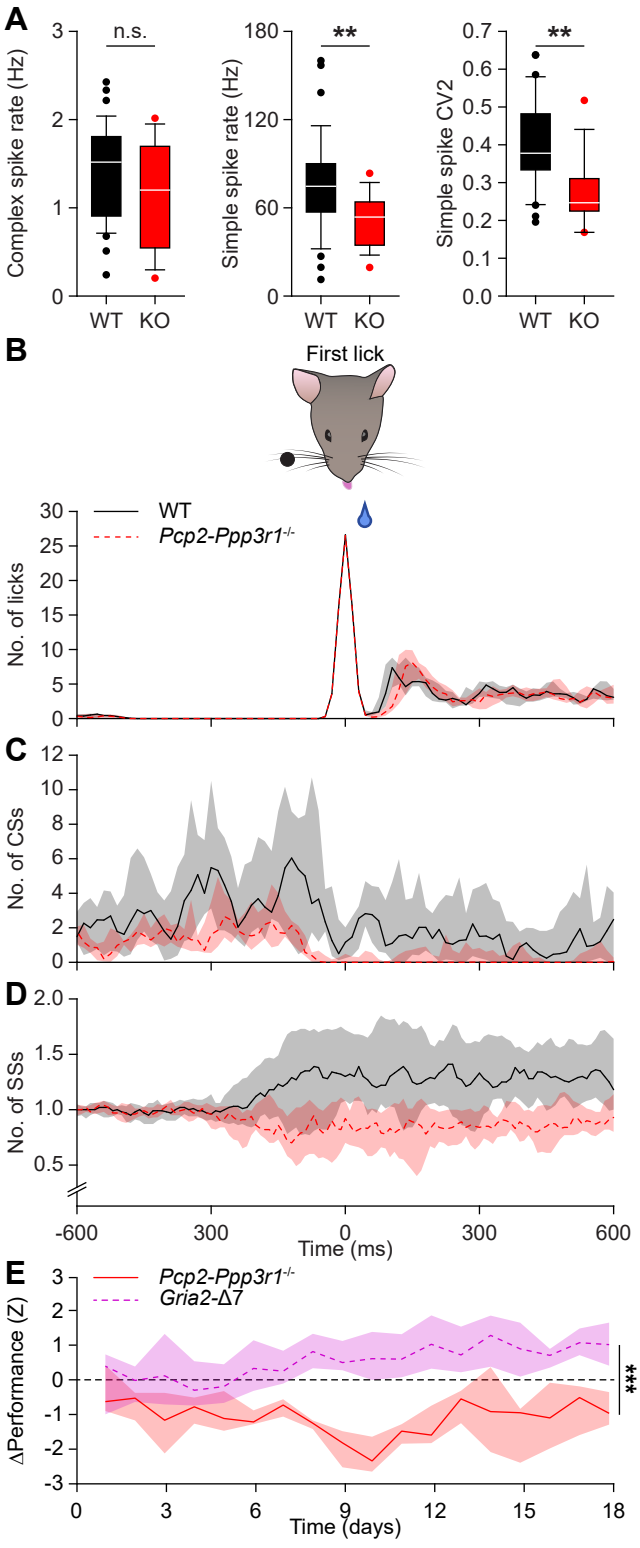

Figure S8. PC responses during trials with licks in Pcp2-Ppp3r1 KO mice. Related to Figure 7.

A. Comparison of the average CS (left) and SS rate (middle) and SS CV2 in WT and *Pcp2-Ppp3r1* KO mice. For statistics, see Table S2. Licks (**B**), CSs (**C**) and SSs (**D**) triggered on the first lick of bouts within the response window of hit trials. Note the decrease in CSs around licking start, as well as the suppressed SS firing during licking in *Pcp2-Ppp3r1* KO mice. **E.** The difference between the fraction of hit trials of *Pcp2-Ppp3r1* KO mice and the one of their control littermates (see Figure 7B) is expressed in Z-score and compared with the one obtained from the learning curves of *Gria2*-Δ7 KI mice and their control littermates. Of the two transgenic mouse lines tested, only *Pcp2-Ppp3r1* KO mice show impaired learning. *Pcp2-Ppp3r1* KO mice performed significantly worse than the *Gria2*-Δ7 KI mice ($p < 0.001$, $F = 47.590$, df = 1, repeated measures ANOVA).

Table S1. Statistical evaluation of CS and SS rates. Related to Figures 3 and S1.

Maximal CS firing (significant cells only) [go trials]								
	n cells	Period 1 [20-100 ms]	*p*	H/W	Period 2 [240-320 ms]	*p*	H/W	Test
p		**0.027** *			**0.016** *			Kruskal-Wallis
H(2)		7.236			8.28			
Naíve mice	16	5.23 (9.71)			0.98 (2.60)			
Non-expert mice	15	3.91 (3.08)	0.659	0.441	3.91 (3.08)	**0.022** *	-2.286	vs. naïve mice
Expert mice	12	1.25 (1.38)	**0.010** *	-2.563	4.60 (1.38)	**0.010** *	2.573	vs. naïve mice
[go vs. no-go trials]								
Naíve mice	16		0.782	12		0.562	24	Wilcoxon
Non-expert mice	15		0.639	-26		0.055	68	Wilcoxon
Expert mice	12		0.339	18		**0.012** *	62	Wilcoxon
Maximal CS firing (all cells) [go trials]								
p		**0.013** *			0.113			Kruskal-Wallis
H(2)		8.757			4.358			
Naíve mice	24	2.66 (5.47)			1.32 (2.41)			
Non-expert mice	20	2.91 (3.18)	0.833	-0.211	2.04 (3.10)	n/a		vs. naïve mice
Expert mice	22	1.25 (1.41)	**0.011** *	-2.513	1.69 (4.03)	n/a		vs. naïve mice
			0.009 *	-2.607		n/a		vs. non-expert
[go vs. no-go trials]								
Naíve mice	24		0.509	48		0.393	58	Wilcoxon
Non-expert mice	20		0.674	24		0.097	129	Wilcoxon
Expert mice	22		0.443	-49		0.036	90	Wilcoxon
SS modulation (all cells) [go trials]								
	n cells	Period A [35-45 ms]	*p*	H/W	Period 1 [95-145 ms]	*p*	H/W	Test
p		0.161			**0.017** *			
H(2)		3.652			8.160			
Naíve mice	24	0.83 (4.15)			4.10 (7.29)			
Non-expert mice	20	0.70 (1.77)	n/a		3.06 (3.69)	0.982	0.023	vs. naïve mice
Expert mice	22	-0.25 (1.97)	n/a		0.85 (1.94)	**0.011** *	-2.538	vs. naïve mice
			n/a			**0.016** *	-2.402	vs. non-expert
[go vs. no-go trials]								
Naíve mice	24		0.603	38		**0.331**	-70	Wilcoxon
Non-expert mice	20		0.133	-39		**0.001** *	168	Wilcoxon
Expert mice	22		0.545	82		**0.824**	-14	Wilcoxon
	n cells	Period B [255-305ms]	*p*	H/W	Period 2 [545-605 ms]	*p*	H/W	Test
p		0.245			**0.009** *			
H(2)		2.814			9.531			
Naíve mice	24	1.73 (3.32)			0.41 (1.21)			
Non-expert mice	20	4.37 (5.24)	n/a		4.07 (8.15)	**0.003** *	-2.958	vs. naïve mice
Expert mice	22	3.81 (6.70)	n/a		5.85 (9.22)	**0.031** *	2.161	vs. naïve mice
			n/a			0.404	-0.834	vs. non-expert
[go vs. no-go trials]								
Naíve mice	24	0.128	-108			0.439	56	Wilcoxon
Non-expert mice	20	**0.024** *	120			**0.011** *	134	Wilcoxon
Expert mice	22	0.198	81			0.028	135	Wilcoxon

Firing rates are normalized to the inter-trial frequency and indicated as median values (interquartile ranges). During period 2 of the SSs, the average value was taken (as this concerned a plateau rather than a peak). Post-hoc tests were only performed if the Kruskall-Wallis test was significant. * indicates significance after Benjamini-Hochberg correction. Note that, for reasons of clarity, in Figure 3D only two time intervals are plotted.

Table S2. Spiking parameters of *Pcp2-Ppp3r1* KO mice. Related to Figure S8A.

	WT (n = 37)	*Pcp2-Pppr3r1* KO (n = 19)	*p*	U	Sign?	Test
CS rate	1.5 (0.8) Hz	1.2 (1.0) Hz	0.081	250	no	Mann-Whitney
SS rate	74.6 (30.37) Hz	53.64 (26.3) Hz	**0.004**	184	yes	Mann-Whitney
SS CV2	0.38 ± 0.14	0.25 ± 0.08	**<0.001**	151	yes	Mann-Whitney

Frequencies and CV2 are indicated as median values (interquartile ranges). Statistical significance (yes or no) is indicated after Bonferroni correction for multiple comparisons.

Table S3. Abbreviations.

CS	complex spike
CV2	local coefficient of variation
Gria2	Glutamate receptor ionotropic AMPA type subunit 2
IQR	inter-quartile range
KI	knock in
KO	knock out
LTD	long-term depression
LTP	long-term potentiation
PC	Purkinje cell
Pcp2	Purkinje cell protein 2 (formerly known as L7)
Ppp3r1	Protein phosphatase 3 regulatory subunit 1 (formerly known as PP2B)
PSTH	peri-stimulus time histogram
Sign	(statistically) significant
SS	simple spike
WT	wild type